plastic containers and the resin lining of cans [4]. Among the known estrogen-like EEDs, BPA has received much attention because it is commonly found in the environment as well as in human tissues and fluids (1–19.4 nM) [4,5]. BPA has been detected in 92% of urine samples in a US reference population, suggesting people may be continuously exposed to this compound in their daily lives [6]. The US Food and Drug Administration and Environmental Protection Agency concluded in the 1980s that a daily dose of 50 μg/kg/day was safe for humans, which is currently considered as $<2.19\times10^{-7}$ M for *in vitro* cell or organ culture studies [7]. However, in recent decades, there has been a heated controversy over the safety of BPA among scientists and risk assessors.

Recently, exposure to BPA at concentrations detected in humans has been reported to affect neurological, cardiovascular and metabolic diseases (such as diabetes), and even cancers [8–12]. However, the effect of low-dose BPA exposure on human reproductive health is still controversial [13,14]. Li *et al.* reported that occupational exposure to BPA has adverse effects on male sexual dysfunction, which is the first evidence that exposure to BPA in the workplace could have an adverse effect on male sexual dysfunction [15]. Jasarevic *et al.* reported that exposure to BPA at low doses can affect sexual behaviors, even with no changes in sexual phenotypes or hormones [16]. Furthermore, Zhang *et al.* reported that low-dose BPA exposure could directly disrupt steroidogenesis in human cells [17]. It seems that exposure to BPA might affect human reproductive health by complicated mechanisms that encompass more than just estrogen receptor (ER) mediated pathways.

In this study, to better understand the molecular basis of the effects of BPA on human reproductive health, a genome-wide screen was performed using human foreskin fibroblast cells (hFFCs) derived from child HS patients to identify novel targets of low-dose BPA exposure. Furthermore, the effect of BPA on the global gene expression profile of hFFCs was compared with that of 17β-estradiol (E2) and 2,3,7,8-tetrachlorodibenzo-p-dioxin (TCDD), which are representative agonists of ER and aryl hydrocarbon receptor (AhR) signaling pathways, respectively.

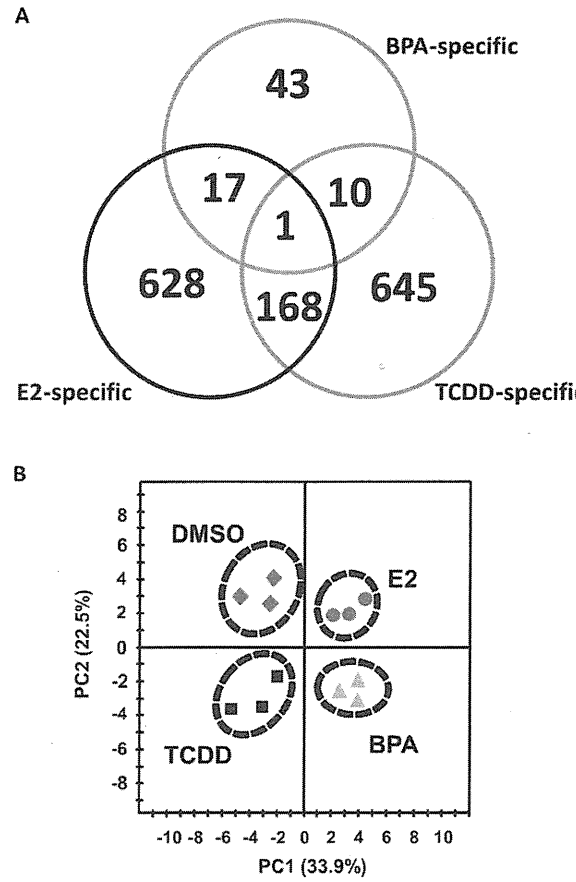

Figure 1. Genetic response of hFFCs to BPA, E2 and TCDD. (*A*) Venn-diagrams showing the number of genes that were considered significantly deregulated among the three treatment groups. (*B*) PCA scoreplot from transcript data of three hFFC cultures treated with DMSO, 10 nM BPA, 0.01 nM E2 and 1 nM TCDD.
doi:10.1371/journal.pone.0036711.g001

Materials and Methods

Samples

hFFCs from child HS ($n=23$; median age 2.3 yrs) and CO ($n=11$; median age 2.3 yrs) patients undergoing surgical procedures were obtained from the National Research Institute for Child Health and Development, Japan, during 2007–2009. All subjects were of Japanese origin and written informed consent was obtained from the guardians on the behalf of the children participants involved in this study. This study was approved by the Institutional Ethics Committees of the Nagoya City University Graduate School of Medical Sciences, the National Research Institute for Child Health and Development and the National Institute for Environmental Studies.

Table 1. Summary of genes differentially expressed in response to BPA, E2 and TCDD.

	BPA		E2		TCDD	
P-value	1.0-fold	1.2-fold	1.0-fold	1.2-fold	1.0-fold	1.2-fold
0.05	154	71*	1101	814*	1150	824*
0.01	30	17	198	154	208	156
0.001	7	5	16	11	14	9

*Selected as significant differentially expressed genes and used for the network generation and pathway analysis.
doi:10.1371/journal.pone.0036711.t001

Chemicals

Dimethyl sulfoxide (DMSO) and E2 were obtained from Sigma Chemical Co. (St. Louis, MO, USA). BPA was obtained from Wako Industries (Osaka, Japan) and TCDD was obtained from Cambridge Isotope Laboratories (Cambridge, MA, USA). DMSO was used as the primary solvent for all chemicals, and the DMSO solutions were further diluted in cell culture media for treatments. The final concentrations of DMSO in media did not exceed 0.1% (vol/vol).

Cell culture

hFFCs were maintained in Dulbecco's Modified Eagle Medium (DMEM)/Ham's F-12 (048-29785, Wako, Osaka, Japan) containing 10% fetal bovine serum (FBS, Mediatech, Herndon, VA, USA) and grown at 37°C in a 5% CO_2 humidified incubator. For growth under steroid-free conditions, cells were seeded in phenol red-free DMEM/Ham's F-12 (045-30665, Wako) containing 5%

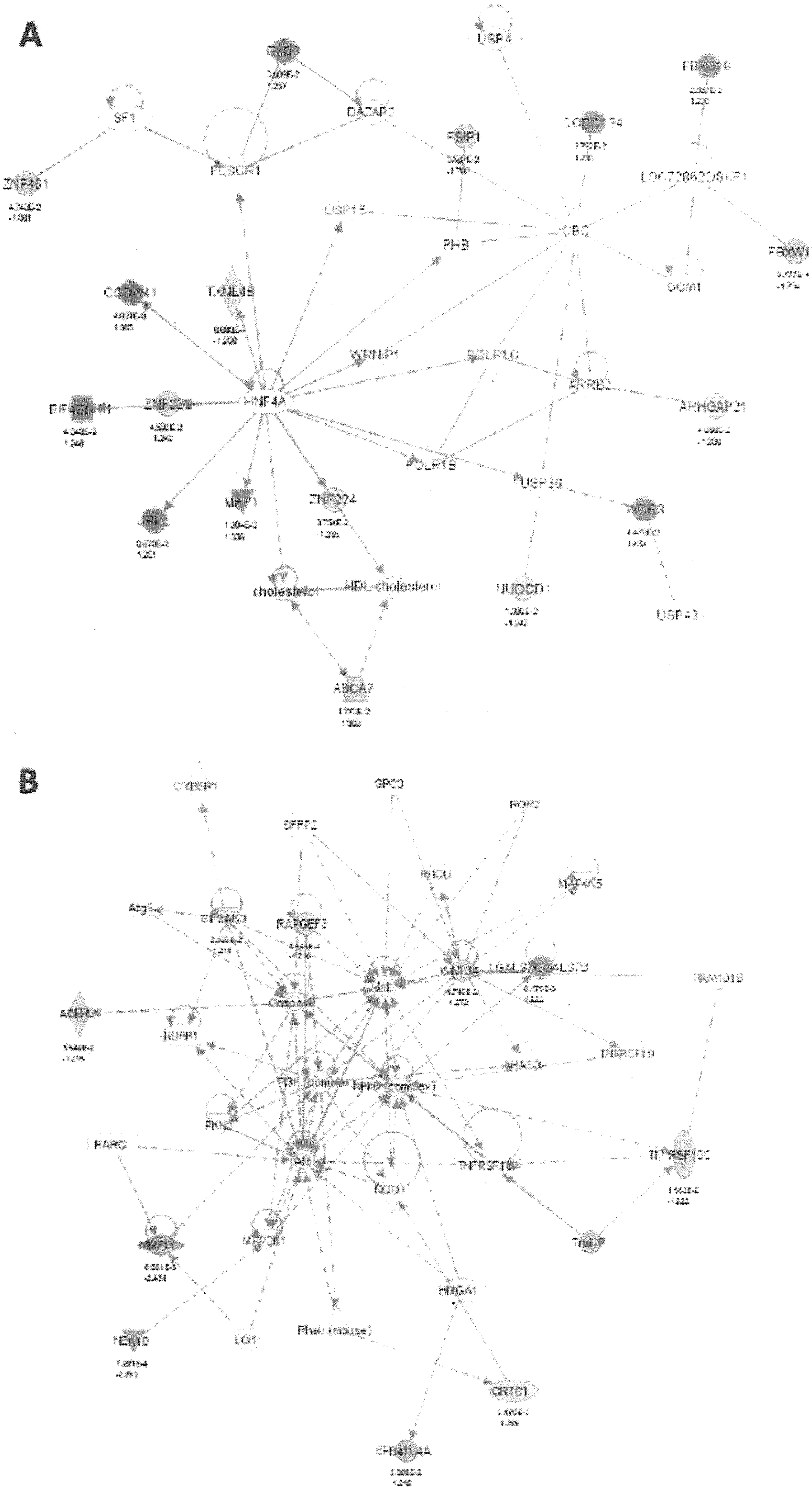
A
USP4
SF1
DAZAP2
FSIP1
ZNF461
USP15
PHB
WRNIP1
HNF4A
ARRB2
ARHGAP21
POLR1B
USP36
ZNF224
cholesterol
HDL cholesterol
NUDCD1
USP43
ABCA7
FBXW12
B
GPC3
ROR2
SFRP2
MAP4K5
Atg5
RAPGEF3
ADRB2
TNFRSF19
TNFRSF10A
EPB41L4A

Figure 2. Network associated genes differentially expressed in response to BPA. (*A*) "Endocrine System Disorders, Gastrointestinal Disease, Genetic Disorder" network and (*B*) "Cell Death, Cellular Growth and Proliferation, Cancer" network. The images were created using the IPA platform by overlaying the differentially expressed genes in response to BPA detected by Agilent microarray analysis onto a global molecular network from the Ingenuity knowledgebase. Red indicates upregulated genes, green indicates downregulated genes, and white indicates genes that were not annotated in this array but that form part of this network. The bottom numbers indicate the fold changes induced by BPA, and the top numbers are the *P*-values between the DMSO control group and the BPA treated group. Direct relationships are exhibited with solid arrows and indirect relationships with dashed arrows.
doi:10.1371/journal.pone.0036711.g002

charcoal/dextran-treated FBS (Hyclone, Logan, UT, USA). All culture media contained 100 U/ml penicillin/streptomycin and 2 mmol/L L-glutamine (Mediatech, Herndon, VA, USA).

RNA isolation and DNA microarray analysis

Total RNA was isolated from cultured cells after treatment with chemicals for 24 h using an RNeasy Kit (Qiagen, Valencia, CA, USA) in accordance with the manufacturer's instructions. Quantification and quality assessment of the isolated RNA samples were performed and verified using an Agilent Bioanalyzer2100 (Agilent Technologies, Palo Alto, CA, USA) and a NanoDrop spectrophotometer (NanoDrop products, Wilmington, DE, USA) in accordance with the manufacturer's instructions. RNA was amplified into cRNA and labeled according to the Agilent One-Color Microarray-Based Gene Expression Analysis protocol (Agilent Technologies). Samples were then hybridized to G4851A SurePrint G3 Human GE 8×60K array slides (60,000 probes, Agilent Technologies). The slides were processed according to the manufacturer's instructions without any modification. The arrays were scanned using an Agilent Microarray Scanner (G2565BA, Agilent Technologies).

MIAME

All data are MIAME compliant, and the raw data have been deposited in the Gene Expression Omnibus (www.ncbi.nlm.nih.gov/geo, accession no. GSE35034).

Array data analysis

The scanned images were analyzed using the standard procedures described in the Agilent Feature Extraction software 9.5.3.1 (Agilent Technologies). Data analysis was performed with GeneSpring GX12.0.2 (Agilent Technologies). Signal intensities for each probe were normalized to the 75th percentile without baseline transformation. Genes that were differentially expressed following chemical treatments were identified by the unpaired Student's t test with P values cut off at 0.05 and fold change of more than 1.2 and were used for the network generation and pathway analysis.

Network generation and pathway analysis

The Ingenuity Pathways Analysis (IPA) program (Ingenuity Systems, Mountain View, CA, USA; http://www.ingenuity.com) was used to identify networks and canonical pathways of genes differentially expressed in response to BPA, E2 and TCDD. IPA software uses an extensive database of functional interactions that are drawn from peer-reviewed publications and manually maintained [18]. For the IPA analysis, the Agilent SurePrint G3 Human GE 8×60 K Array was used as a reference gene set. The generated biological networks were ranked by score, which is the likelihood of a set of genes being found in the networks owing to random chance, identified by a Fisher's exact test. The generated canonical pathways were ranked by P values, which is calculated using a Fisher's exact test by comparing the number of user-specified genes of interest that participate in a given function or pathway, relative to the total number of occurrences of these genes in all functional/pathway annotations stored in the Ingenuity

Table 2. Top five associated network functions of genes differentially expressed in response to BPA, E2 and TCDD generated by IPA.

Chemical	Top Functions	Score
BPA	Endocrine System Disorders, Gastrointestinal Disease, Genetic Disorder	41
	Cell Death, Cellular Growth and Proliferation, Cancer	21
	Cellular Growth and Proliferation, Hematological System Development and Function, Cellular Development	18
	Cellular Assembly and Organization, Cellular Function and Maintenance, Cell Cycle	13
	Dermatological Diseases and Conditions, Inflammatory Disease	3
E2	Cellular Growth and Proliferation, Skeletal and Muscular System Development and Function, Cell Cycle	41
	DNA Replication, Recombination, and Repair, Gene Expression, Cellular Assembly and Organization	41
	Cellular Assembly and Organization, Cellular Function and Maintenance, Protein Synthesis	41
	Gene Expression, Cell Cycle, Cell-To-Cell Signaling and Interaction	35
	DNA Replication, Recombination, and Repair, Nucleic Acid Metabolism, Small Molecule Biochemistry	33
TCDD	Post-Translational Modification, Genetic Disorder, Hematological Disease	49
	Cell Cycle, Cellular Assembly and Organization, DNA Replication, Recombination, and Repair	47
	Cellular Assembly and Organization, DNA Replication, Recombination, and Repair, Decreased Levels of Albumin	45
	DNA Replication, Recombination, and Repair, Energy Production, Nucleic Acid Metabolism	44
	DNA Replication, Recombination, and Repair, Cell Cycle, Cellular Assembly and Organization	37

doi:10.1371/journal.pone.0036711.t002

Table 3. Top canonical pathways for genes differentially expressed in response to BPA, E2 and TCDD identified by IPA.

Chemical	Top canonical pathway	P-Value
BPA	RAN Signaling	5.31E-02
	Endoplasmic Reticulum Stress Pathway	6.34E-02
	Leukocyte Extravasation Signaling	1.24E-01
	Retinoic acid Mediated Apoptosis Signaling	1.54E-01
	Colorectal Cancer Metastasis Signaling	1.93E-01
E2	Cell Cycle: G1/S Checkpoint Regulation	1.01E-03
	PI3K/AKT Signaling	1.52E-03
	Role of NFAT in Regulation of the Immune Response	1.83E-03
	p53 Signaling	3.46E-03
	Aryl Hydrocarbon Receptor Signaling	3.63E-03
TCDD	Cell Cycle Control of Chromosomal Replication	1.20E-09
	Role of BRCA1 in DNA Damge Response	1.72E-07
	Mismatch Repair in Eukaryotes	2.47E-05
	Hereditary Breast Cancer Signaling	9.45E-04
	Role of CHK Proteins in Cell Cycle Checkpoint Control	1.00E-02

doi:10.1371/journal.pone.0036711.t003

Pathways Knowledge Base [19]. In addition, genes significantly differentially expressed in response to BPA, E2 and TCDD was analyzed by Pathway Express (http://vortex.cs.wayne.edu/projects.htm) and mapped to Kyoto Encyclopedia of Genes and Genomes (KEGG) pathways by KegArray (http://www.kegg.jp/kegg/download/kegtools.html).

Quantitative real-time reverse-transcription polymerase chain reaction (RT-PCR)

cDNA was synthesized using a High Capacity RNA-to-cDNA Kit (Applied Biosystems, Foster City, CA, USA) according to the manufacturer's instructions. Real-time PCR was performed using TaqMan® Gene Expression Master Mix (Applied Biosystems) in accordance with the manufacturer's instructions. TaqMan® Gene Expression Assays (Applied Biosystems) used in this study were: Hs02341150_m1 for POMZP3, Hs01094348_m1 for WDR3, Hs00171829_m1 for metallopeptidase 11 (MMP11; see gene names in Table S1), and Hs00266705 g1 for glyceraldehyde-3-phosphate dehydrogenase (GAPDH). The primers (Forward: 5′-TGTTGGGGGATAAGGACAAA-3′; and Reverse: 5′-GCAGGCTGTACAGGAACCAT-3′) and probe (5′-TAAACT-CACCTCTGTGGTTGGAACAAT-3′) for NEK10 were designed and synthesized by Hokkaido System Science (Sapporo, Hokkaido, Japan). The amplification reaction was performed in an ABI PRISM 7000 Sequence Detector (Applied Biosystems) under the following cycling conditions: 95°C for 15 min, followed by 40 cycles of 95°C for 15 s and 60°C for 60 s. The gene expression levels were calculated based on the threshold cycle using Sequence Detection System Software (Applied Biosystems). Gene expression was normalized to that of GAPDH and set to 100 for the control DMSO-treated cells.

Statistical and multivariate analysis

Quantitative data were expressed as the mean ± SEM. A nonparametric test, the Mann-Whitney U test, was applied to test for statistical significance. Values of $P<0.05$ were considered to indicate statistical significance. Unsupervised principal component analysis (PCA) was run in SIMCA-P+ (Version 12.0, Umetrics, Umeå, Sweden) to obtain a general overview of the variance of genes differentially expressed in response to BPA, E2 and TCDD.

Results

Gene expression profiles of hFFCs in response to BPA, E2 and TCDD

The gene expression profiles in hFFCs treated with DMSO control or 10 nM BPA, 0.01 nM E2 or 1 nM TCDD were determined by Agilent microarray analysis using three biological replicates. Then, differentially expressed genes in response to BPA, E2 and TCDD compared with DMSO control were identified by the unpaired Student's t test with P values cut off at 0.05 and fold change of more than 1.2 using GeneSpring GX software. Seventy-one genes (42 downregulated and 29 upregulated), 814 genes (371 downregulated and 443 upregulated), and 824 genes (344 downregulated and 480 upregulated) were identified to be significantly differentially expressed in response to BPA, E2, and TCDD, respectively. No nuclear receptor was found to be significantly differentially expressed in response to BPA, while estrogen-related receptor-α (ESRRA), retinoic acid receptor-α (RARA) and RAR-related orphan receptor-α (RORA) and RARA were found to be significantly differentially expressed in response to E2 and TCDD, respectively. The summary of differentially expressed genes along with their P values and fold changes is provided in Table 1.

Differences in the response of hFFCs to BPA, E2 and TCDD

Comparison of the gene expression profiles of hFFCs in response to BPA, E2 and TCDD is provided in Figure 1. BPA-specific responses were found in 43 significantly differentially expressed genes, compared with responses to E2 and TCDD (Figure 1A). Seventeen and 10 differentially expressed genes were found to be common in response to BPA with E2 or TCDD, respectively. A full list of these genes is summarized in Table S1.

Furthermore, to compare the expression patterns of hFFCs in response to BPA with that of E2 or TCDD, PCA analysis was performed on the data of significantly differentially expressed genes in response to BPA. PCA is a standard technique of pattern recognition and multivariate data analysis. Of interest, the cells treated with DMSO, BPA, E2 and TCDD were clearly distinguished from each other by the PCA score plots (Figure 1B). According to the first component (PC1), which represents 33.9% of the total variance, a very clear discrimination between cells treated with BPA or E2 and those treated with DMSO or TCDD was observed. However, according to the second component (PC2), which represents 22.5% of the total variance, cells treated with BPA or TCDD were clearly distinguished from those treated with DMSO or E2. It should be noted that differences in the PCA were identified using an unsupervised analysis, without any prior information on the samples. Since all cells were cultured under identical conditions, the observed discriminations demonstrate that the effect of BPA is similar to that of E2 according to PC1 but is similar to that of TCDD according to PC2.

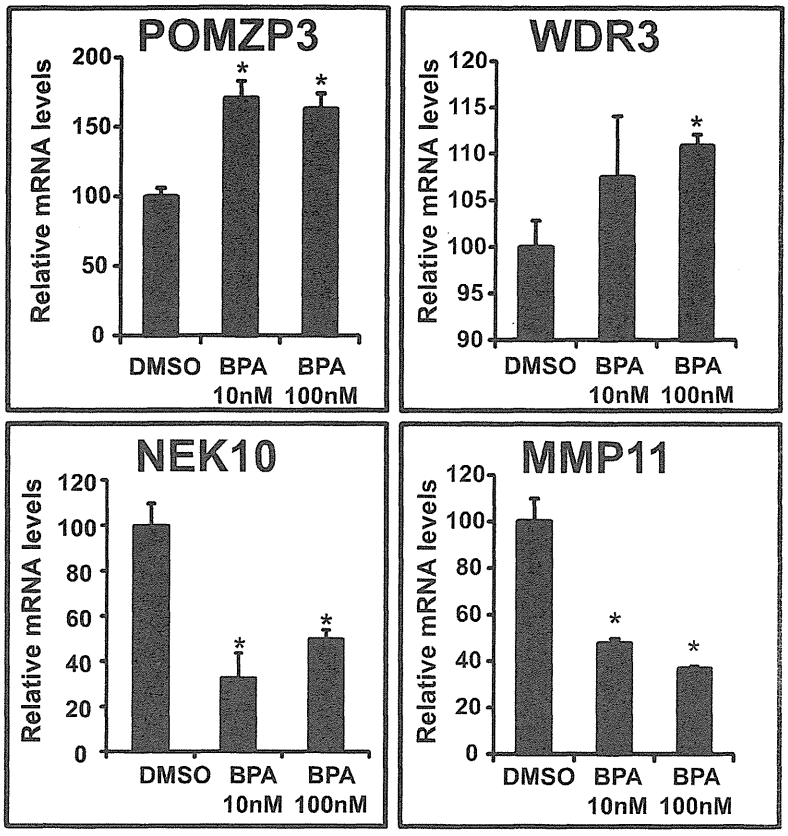

Figure 3. Validation of POMZP1, WDR3, NEK10 and MMP11 expression. Cells were treated with BPA at 10 nM and 100 nM for 24 h, and then the expression of POMZP1, WDR3, NEK10 and MMP11 was examined by real-time PCR. *$P<0.05$ vs. DMSO control cells.
doi:10.1371/journal.pone.0036711.g003

Network generation and pathway analysis of genes differentially expressed in response to BPA, E2 and TCDD

To investigate possible biological interactions of differently regulated genes, datasets derived from microarray analysis representing genes with altered expression profiles were imported into the IPA platform. Network analysis of the biological functions of the top five IPA-generated networks is summarized in Table 2 and is shown in Figure 2 and Figure S1,S2,S3.The two most highly populated biological networks entitled "Endocrine System Disorders, Gastrointestinal Disease, Genetic Disorder" (Score = 41) and "Cell Death, Cellular Growth and Proliferation, Cancer" (Score = 21) were identified with genes differentially expressed in response to BPA (Figure 2). The networks consisted of genes that encoded enzymes (ACER2, PLSCR1, POLR1C, TXNL4B and UBC), peptidases (MMP11, UCHL5, USP4, USP36 and USP43), proteins that regulate transcription (ABCA7, CRTC1, HNF4A, LOC728622/SKP1, PHB, SF1 and SLC25A6) and translation (EIF4ENIF1 and TNFRSF10C), and others (ARHGAP21, ARRB2, CCDC41, CCDC134, EIF2AK3, EPB41L4A, DAZAP2, EPB41L3, EXD3, FBXO18, FBXW12, FSIP1, JRKL, LGALS7/LGALS7B, NEK10, NUDCD1, RAPGEF3, SERPINA1, WDR3, WNT3A, ZNF222, ZNF224 and ZNF461). The most highly populated biological networks were identified with genes differentially expressed in response to E2 and TCDD and were entitled "Cellular Growth and Proliferation, Skeletal and Muscular System Development and Function, Cell Cycle" (Score = 41) and "Post-Translational Modification, Genetic Disorder, Hematological Disease" (Score = 49), respectively. Furthermore, top canonical pathways associated with genes significantly differentially expressed in response to BPA, E2 and TCDD were summarized in Table 3. The pathway most affected by BPA is "RAN Signaling" with only borderline significance ($P = 0.0531$). The pathways most affected by E2 and TCDD are "Cell Cycle: G1/S Checkpoint Regulation" and "Cell Cycle Control of Chromosomal Replication", respectively ($P = 1.01\times10^{-3}$ and 1.20×10^{-9}, respectively).

In addition, a list of top KEGG pathways affected by BPA, E2 and TCDD identified by Pathway Express was summarized in Table S2. By inputting the list of genes significantly differentially expressed in response to BPA, E2 and TCDD into Pathway Express, 12 KEGG pathways, but without statistical significance, were found to be affected by BPA, while 27 and 9 KEGG pathways were found to be significantly affected by E2 and TCDD, respectively. As an example, "Pathways in cancer" of KEGG mapped with genes significantly differentially expressed in response to BPA, E2 and TCDD using KegArray was illustrated in Figure S4.

Validation by real-time PCR

To validate the microarray data and to identify potential biomarkers for BPA toxicity in hFFCs derived from HS patients, the expression of the most up- or down-regulated genes (POMZP3, 1.46-fold; WDR3, 1.45-fold; NEK10, 0.44-fold;

A

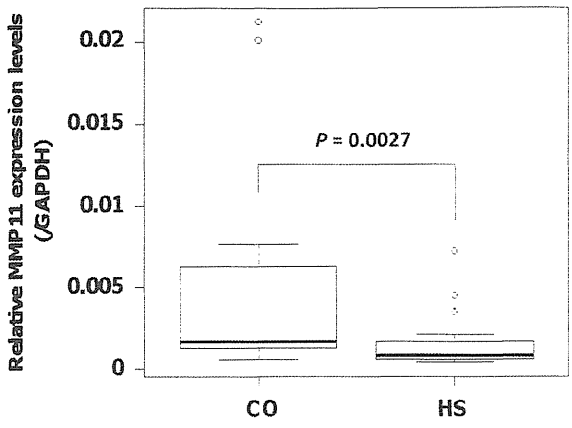

B

	n	Relative MMP11 expression levels (/GAPDH) (mean ± SEM)
CO	11	0.0058 ± 0.0022
HS	23	0.0015 ± 0.00033

Figure 4. Reduced levels of MMP11 expression in hFFCs derived from child HS patients. Significantly lower MMP11 expression was observed in hFFCs derived from the HS ($n = 23$) group compared with the CO ($n = 11$) group by TaqMan real-time PCR. (*A*) Boxplot and (*B*) summary of the quantitative data comparing MMP11 expression levels in HS and CO groups.
doi:10.1371/journal.pone.0036711.g004

MMP11, 0.41-fold) in response to BPA was validated by real-time PCR. As the results show in Figure 3, the PCR data showed good concordance with the microarray data in terms of the expression direction (up- or down-regulation). A significant increase in the mRNA levels of POMZP3 and WDR3 and a significant decrease in the mRNA levels of NEK10 and MMP11 were observed following BPA treatments at high and/or low concentrations (10 nM and 100 nM, respectively).

Comparison of MMP11 expression levels in hFFCs derived from child HS and CO patients

To further investigate the potential role of MMP11 in the development of HS, we examined the expression levels of MMP11 in hFFCs derived from child HS and CO patients ($n = 23$ and 11, respectively). As shown Figure 4, the mean MMP11 expression level, normalized to GAPDH, in the HS group was 0.0015 and in the CO group, 0.0058. Significantly lower MMP11 expression levels were observed in the HS group compared with the CO group (0.25-fold, $P = 0.0027$).

Discussion

To better understand the molecular basis of the effects of BPA on human reproductive health, target genes of low-dose BPA exposure were identified in hFFCs derived from child HS patients using DNA microarray analysis. Human foreskin tissues obtained from patients with HS have been used as *in vitro* models to define the etiology of HS [20–22]. However, these investigations have not delineated the relative contribution of environmental factors. To our knowledge, our study is the first report to use hFFCs to investigate the potential effects of BPA on the development of HS. The concentration of BPA used to treat the cells in our microarray analysis was 10 nM, which is below the dose of 50 μg/kg/day (approximately 200 nM for *in vitro* cell or organ culture studies) usually considered as safe for humans [7]. Moreover, this dose is in the concentration range of 1–19.4 nM that is commonly detected in human tissues and fluids [4].

In this study, we compared the gene expression profiles of hFFCs in response to BPA, E2 and TCDD. Using PCA, we found that the effect of BPA is similar to that of E2 according to PC1 but is similar to that of TCDD according to PC2. Forty-three genes were found to be affected exclusively by BPA, underscoring the concept that the effects observed are ER and AhR-independent (Figure 1). In our previous study, we examined the estrogenic activity of BPA in estrogen receptor 1 (ESR1)-positive BG1Luc4E2 human ovarian cancer cells and found that BPA increased the ESR1-induced luciferase activity in a dose-dependent manner with a lowest observed effect at 100 nM [23]. Although differences exist between cell lines, it is possible that the underlying mechanisms of the endocrine-disrupting effects of BPA at doses lower than the reference limits might involve pathways other than estrogen signaling. Indeed, differences in transcript profiles in response to BPA and E2 have been previously described in ESR1-positive human cells [24]. Furthermore, amore recent study reported that BPA might lead to severe malformation during vertebrate embryogenesis, while no effects were seen with exposure to the E2 or ER-antagonist ICI 182,780 [25].

It is not unexpected that the largest biological network identified by IPA analysis with genes differentially expressed in response to BPA was entitled "Endocrine System Disorders, Gastrointestinal Disease, Genetic Disorder" (Table 2 and Figure 2A). It should be noted that this network contains three genes (ZNF222, ZNF224 and ZNF461) that belong to the zinc finger protein (ZFP) family. ZFPs are among the most abundant proteins in eukaryotic genomes and play various roles in the regulation of transcription [26]. The biological function of ZNF222 and ZNF461 remains to be investigated, but ZNF224 participates in key cellular processes, such as regulation of cell growth [27]. Previous reports have revealed that ZNF224 might play a critical role in bladder carcinogenesis by regulating the apoptosis of bladder cancer cells [28]. None of these three ZNFs have been previously associated with the development of HS. However, two other zinc finger box genes, ZEB1 and ZEB2, have been associated with HS [20,29]. Our data indicate that ZFP-mediated transcriptional activity might be required for the effect of BPA on human reproduction. It is known that zinc finger structures are as diverse as their functions [26]. Therefore, it is likely that further investigations into the function of ZFPs in transcriptional regulation will provide novel insights to explain the association we found between ZFP expression and low-dose BPA exposure regarding the pathogenesis of HS.

The expression of four of the significantly differentially expressed genes identified in the microarray analysis was verified by real-time PCR analysis. Of particular interest, MMP11 (0.47-fold and 0.37-fold at 10 nM and 100 nM, respectively), which is involved in the "Cell Death, Cellular Growth and Proliferation, Cancer" network, was shown to be down-regulated (Figures 2B and 3). The matrix metalloproteinases (MMPs) are zinc-dependent endopeptidases that are involved in the breakdown of extracellular matrix (ECM) in normal physiological processes, such as embryonic development, reproduction, and tissue remodeling, as well as in disease processes, such as arthritis and metastasis [30,31]. It is well known that MMP11 is overexpressed in several human cancers, including breast, cervix, colon, ovary, prostate,

and stomach cancers [30,32–34]. Several MMPs have been implicated in ECM degradation associated with tumor growth and angiogenesis, which is required for a cancer cell to invade a nearby blood vessel (intravasation) and then to extravasate at a distant location and invade the distant tissue in order to seed a new metastatic site [35].

To our knowledge, there have not been any reports of human congenital genital disorders associated with MMP11. However, it has been reported that MMPs play a critical role in cell fate and behavior during many developmental processes [31,36]. Both genetic analysis using transgenic mice and pharmacogenetic studies with chemical inhibitors have elucidated that loss of function of MMPs, in particular MMP11, might induce dysregulation in cell migration and apoptosis during tissue remodeling or branching of mammary epithelial cells [37,38]. A more recent study in the model insect, *Tribolium*, explored MMP functions *in vivo* and found that knockdown of MMPs using genetic interference resulted in malformation in tracheal and gut development during beetle embryogenesis and pupal morphogenesis [39]. It is known that epithelial seam formation and remodeling during urethral formation play important roles in the etiology of HS. The urethral abnormalities seen in HS can be viewed as a failure of epithelial cell adhesion [40]. Therefore, we hypothesized that downregulation of MMP11 expression might decrease cellular adhesion in the developing male urethra and ventral penile skin, which might result in the abortive penile development seen in HS.

To further confirm this hypothesis, we compared the expression levels of MMP11 in hFFCs derived from child HS and CO patients ($n = 23$ and 11, respectively). In 2001, Skakkebaek and his colleagues proposed a concept of TDS: impaired development of fetal testes could lead to increased risks of CO, HS, decreased spermatogenesis or testicular cancer [2]. However, they have recently changed their opinion and now suggest that HS is only marginally associated with TDS [3]. Although much remains to be determined, it is likely that the molecular etiology of HS and CO is different. CO is the absence of one or both testes from the scrotum and is the most common congenital abnormality in boys with a reported prevalence at birth of approximately 2–9%, according to registry data [41]. Impaired descent of the testes is thought to be fetal in origin, and if the *in utero* development of the testicles is impaired then their production of insulin-like factor 3 and especially testosterone may be reduced, which may lead to some degree of CO [3,42]. However, it is likely that isolated HS may have a different etiological mechanism, including a congenital developmental problem restricted to the penis [43]. Rey *et al.* found that most boys (85%) with isolated HS had, in general, normal testicular endocrinology in contrast to those with HS combined with other genital abnormalities [44]. In this study, only child HS and CO patients without other genital malformations of syndromes were recruited. Therefore, hFFCs derived from foreskin tissues of child CO patients might be viewed as the control group in this study. We found that MMP11 expression in the HS group was significantly lower than in the CO group (0.25-fold, $P = 0.0027$) (Figure 4). This result is in accordance with our hypothesis that downregulation of MMP11 expression might be related with the pathology of HS. Although the urethral tissue was not directly examined, it is possible that there is also a potential effect of MMP11 on urethral development.

In summary, the present study examined targets of low-dose BPA exposure and transcriptome differences in response to BPA, E2 and TCDD in hFFCs derived from child HS patients using DNA microarray analysis. Of particular interest, the expression of MMP11 was found to be downregulated by BPA in a dose-dependent manner. Furthermore, we also found that MMP11 expression in the HS group was significantly lower than in the CO group. Our findings suggested that the involvement of BPA in the development of HS might relate to downregulation of MMP11 expression. Further study of the novel target genes identified in this study during genital tubercle development might increase our knowledge of the molecular basis of the effects of BPA on human reproductive health.

Supporting Information

Figure S1 Red indicates upregulated genes, green indicates downregulated genes, and white indicates genes that were not annotated in this array but form part of this network. The bottom numbers indicate the fold changes induced by BPA and the top numbers is the P-values between DMSO control group and BPA treated group. (***A***) "Cellular Growth and Proliferation, Hematological System Development and Function, Cellular Development" network; (***B***) "Cellular Assembly and Organization, Cellular Function and Maintenance, Cell Cycle" network.
(DOCX)

Figure S2 Red indicates upregulated genes, green indicates downregulated genes, and white indicates genes that were not annotated in this array but form part of this network. The bottom numbers indicate the fold changes induced by E2 and the top numbers is the P-values between DMSO control group and E2 treated group. (***A***) "Cellular Growth and Proliferation, Skeletal and Muscular System Development and Function, Cell Cycle" network; (***B***) "DNA Replication, Recombination, and Repair, Gene Expression, Cellular Assembly and Organization" network; (***C***) "Cellular Assembly and Organization, Cellular Function and Maintenance, Protein Synthesis" network; (***D***) "Gene Expression, Cell Cycle, Cell-To-Cell Signaling and Interaction" network; (***E***) "DNA Replication, Recombination, and Repair, Nucleic Acid Metabolism, Small Molecule Biochemistry" network.
(DOCX)

Figure S3 Red indicates upregulated genes, green indicates downregulated genes, and white indicates genes that were not annotated in this array but form part of this network. The bottom numbers indicate the fold changes induced by TCDD and the top numbers is the P-values between DMSO control group and TCDD treated group. (***A***) "Post-Translational Modification, Genetic Disorder, Hematological Disease" network; (***B***) "Cell Cycle, Cellular Assembly and Organization, DNA Replication, Recombination, and Repair" network; (***C***) "Cellular Assembly and Organization, DNA Replication, Recombination, and Repair, Decreased Levels of Albumin" network; (***D***) "DNA Replication, Recombination, and Repair, Energy Production, Nucleic Acid Metabolism" network; (***E***) "DNA Replication, Recombination, and Repair, Cell Cycle, Cellular Assembly and Organization" network.
(DOCX)

Figure S4 "Pathways in cancer" of KEGG was mapped with genes significantly differentially expressed in response to BPA (*A*), E2 (*B*) and TCDD (*C*).
(DOCX)

Table S1 Comparison of the gene expression profiles of hFFCs in response to BPA, E2 and TCDD.
(DOCX)

Table S2 KEGG pathways affected by BPA, E2 and TCDD identified by Pathway Express.
(DOCX)

Acknowledgments

The authors gratefully acknowledge critical advices of Dr. Jun Kanno (National Institute of Health Sciences, Japan) and Dr. Yasunobu Aoki (National Institute for Environmental Studies, Japan).

Author Contributions

Conceived and designed the experiments: TF J. Yoshinaga J. Yonemoto MF TO HS. Performed the experiments: XYQ HZ HA QZ. Analyzed the data: XYQ. Contributed reagents/materials/analysis tools: YK K. Mizuno KU K. Muroya MM KK YH MF TO. Wrote the paper: XYQ HS.

References

1. Toppari J, Virtanen HE, Main KM, Skakkebaek NE (2010) Cryptorchidism and hypospadias as a sign of testicular dysgenesis syndrome (TDS): environmental connection. Birth Defects Res A Clin Mol Teratol 88: 910–919.
2. Skakkebaek NE, Rajpert-De Meyts E, Main KM (2001) Testicular dysgenesis syndrome: an increasingly common developmental disorder with environmental aspects. Hum Reprod 16: 972–978.
3. Jorgensen N, Meyts ER, Main KM, Skakkebaek NE (2010) Testicular dysgenesis syndrome comprises some but not all cases of hypospadias and impaired spermatogenesis. Int J Androl 33: 298–303.
4. Vandenberg LN, Hauser R, Marcus M, Olea N, Welshons WV (2007) Human exposure to bisphenol A (BPA). Reprod Toxicol 24: 139–177.
5. Krishnan AV, Stathis P, Permuth SF, Tokes L, Feldman D (1993) Bisphenol-A: an estrogenic substance is released from polycarbonate flasks during autoclaving. Endocrinology 132: 2279–2286.
6. Calafat AM, Kuklenyik Z, Reidy JA, Caudill SP, Ekong J, et al. (2005) Urinary concentrations of bisphenol A and 4-nonylphenol in a human reference population. Environ Health Perspect 113: 391–395.
7. Wetherill YB, Akingbemi BT, Kanno J, McLachlan JA, Nadal A, et al. (2007) In vitro molecular mechanisms of bisphenol A action. Reprod Toxicol 24: 178–198.
8. Allard P, Colaiacovo MP (2010) Bisphenol A impairs the double-strand break repair machinery in the germline and causes chromosome abnormalities. Proc Natl Acad Sci U S A 107: 20405–20410.
9. Leranth C, Hajszan T, Szigeti-Buck K, Bober J, MacLusky NJ (2008) Bisphenol A prevents the synaptogenic response to estradiol in hippocampus and prefrontal cortex of ovariectomized nonhuman primates. Proc Natl Acad Sci U S A 105: 14187–14191.
10. Lang IA, Galloway TS, Scarlett A, Henley WE, Depledge M, et al. (2008) Association of urinary bisphenol A concentration with medical disorders and laboratory abnormalities in adults. JAMA 300: 1303–1310.
11. Wei J, Lin Y, Li Y, Ying C, Chen J, et al. (2011) Perinatal exposure to bisphenol A at reference dose predisposes offspring to metabolic syndrome in adult rats on a high-fat diet. Endocrinology 152: 3049–3061.
12. Qin XY, Fukuda T, Yang L, Zaha H, Akanuma H, et al. (2012) Effects of bisphenol A exposure on the proliferation and senescence of normal human mammary epithelial cells. Cancer Biol Ther 13.
13. Sharpe RM (2010) Is it time to end concerns over the estrogenic effects of bisphenol A? Toxicol Sci 114: 1–4.
14. Welshons WV, Nagel SC, vom Saal FS (2006) Large effects from small exposures. III. Endocrine mechanisms mediating effects of bisphenol A at levels of human exposure. Endocrinology 147: S56–69.
15. Li D, Zhou Z, Qing D, He Y, Wu T, et al. (2010) Occupational exposure to bisphenol-A (BPA) and the risk of self-reported male sexual dysfunction. Hum Reprod 25: 519–527.
16. Jasarevic E, Sieli PT, Twellman EE, Welsh TH, Jr., Schachtman TR, et al. (2011) Disruption of adult expression of sexually selected traits by developmental exposure to bisphenol A. Proc Natl Acad Sci U S A 108: 11715–11720.
17. Zhang X, Chang H, Wiseman S, He Y, Higley E, et al. (2011) Bisphenol A disrupts steroidogenesis in human H295R cells. Toxicol Sci 121: 320–327.
18. Calvano SE, Xiao W, Richards DR, Felciano RM, Baker HV, et al. (2005) A network-based analysis of systemic inflammation in humans. Nature 437: 1032–1037.
19. Bronner IF, Bochdanovits Z, Rizzu P, Kamphorst W, Ravid R, et al. (2009) Comprehensive mRNA expression profiling distinguishes tauopathies and identifies shared molecular pathways. PLoS One 4: e6826.
20. Qiao L, Tasian GE, Zhang H, Cunha GR, Baskin L (2011) ZEB1 is estrogen responsive in vitro in human foreskin cells and is over expressed in penile skin in patients with severe hypospadias. J Urol 185: 1888–1893.
21. Vottero A, Minari R, Viani I, Tassi F, Bonatti F, et al. (2011) Evidence for epigenetic abnormalities of the androgen receptor gene in foreskin from children with hypospadias. J Clin Endocrinol Metab 96: E1953–1962.
22. Wang Z, Liu BC, Lin GT, Lin CS, Lue TF, et al. (2007) Up-regulation of estrogen responsive genes in hypospadias: microarray analysis. J Urol 177: 1939–1946.
23. Qin XY, Zaha H, Nagano R, Yoshinaga J, Yonemoto J, et al. (2011) Xenoestrogens down-regulate aryl-hydrocarbon receptor nuclear translocator 2 mRNA expression in human breast cancer cells via an estrogen receptor alpha-dependent mechanism. Toxicol Lett 206: 152–157.
24. Singleton DW, Feng Y, Yang J, Puga A, Lee AV, et al. (2006) Gene expression profiling reveals novel regulation by bisphenol-A in estrogen receptor-alpha-positive human cells. Environ Res 100: 86–92.
25. Gibert Y, Sassi-Messai S, Fini JB, Bernard L, Zalko D, et al. (2011) Bisphenol A induces otolith malformations during vertebrate embryogenesis. BMC Dev Biol 11: 4.
26. Laity JH, Lee BM, Wright PE (2001) Zinc finger proteins: new insights into structural and functional diversity. Curr Opin Struct Biol 11: 39–46.
27. Lupo A, Cesaro E, Montano G, Izzo P, Costanzo P (2011) ZNF224: Structure and role of a multifunctional KRAB-ZFP protein. Int J Biochem Cell Biol 43: 470–473.
28. Harada Y, Kanehira M, Fujisawa Y, Takata R, Shuin T, et al. (2010) Cell-permeable peptide DEPDC1-ZNF224 interferes with transcriptional repression and oncogenicity in bladder cancer cells. Cancer Res 70: 5829–5839.
29. Garavelli L, Cerruti-Mainardi P, Virdis R, Pedori S, Pastore G, et al. (2005) Genitourinary anomalies in Mowat-Wilson syndrome with deletion/mutation in the zinc finger homeo box 1B gene (ZFHX1B). Report of three Italian cases with hypospadias and review. Horm Res 63: 187–192.
30. Peruzzi D, Mori F, Conforti A, Lazzaro D, De Rinaldis E, et al. (2009) MMP11: a novel target antigen for cancer immunotherapy. Clin Cancer Res 15: 4104–4113.
31. Vu TH, Werb Z (2000) Matrix metalloproteinases: effectors of development and normal physiology. Genes Dev 14: 2123–2133.
32. Valdivia A, Peralta R, Matute-Gonzalez M, Garcia Cebada JM, Casasola I, et al. (2011) Co-expression of metalloproteinases 11 and 12 in cervical scrapes cells from cervical precursor lesions. Int J Clin Exp Pathol 4: 674–682.
33. McCord LA, Li F, Rosewell KL, Brannstrom M, Curry TE, Jr. (2011) Ovarian Expression and Regulation of the Stromelysins During the Periovulatory Period in the Human and the Rat. Biol Reprod.
34. Desmedt C, Majjaj S, Kheddoumi N, Singhal SK, Haibe-Kains B, et al. (2012) Characterization and Clinical Evaluation of CD10+ Stroma Cells in the Breast Cancer Microenvironment. Clin Cancer Res 18: 1004–1014.
35. Roy R, Yang J, Moses MA (2009) Matrix metalloproteinases as novel biomarkers and potential therapeutic targets in human cancer. J Clin Oncol 27: 5287–5297.
36. Wei L, Shi YB (2005) Matrix metalloproteinase stromelysin-3 in development and pathogenesis. Histol Histopathol 20: 177–185.
37. Ishizuya-Oka A, Li Q, Amano T, Damjanovski S, Ueda S, et al. (2000) Requirement for matrix metalloproteinase stromelysin-3 in cell migration and apoptosis during tissue remodeling in Xenopus laevis. J Cell Biol 150: 1177–1188.
38. Simian M, Hirai Y, Navre M, Werb Z, Lochter A, et al. (2001) The interplay of matrix metalloproteinases, morphogens and growth factors is necessary for branching of mammary epithelial cells. Development 128: 3117–3131.
39. Knorr E, Schmidtberg H, Vilcinskas A, Altincicek B (2009) MMPs regulate both development and immunity in the tribolium model insect. PLoS One 4: e4751.
40. Baskin LS, Erol A, Jegatheesan P, Li Y, Liu W, et al. (2001) Urethral seam formation and hypospadias. Cell Tissue Res 305: 379–387.
41. Virtanen HE, Bjerknes R, Cortes D, Jorgensen N, Rajpert-De Meyts E, et al. (2007) Cryptorchidism: classification, prevalence and long-term consequences. Acta Paediatr 96: 611–616.
42. Kojima Y, Mizuno K, Kohri K, Hayashi Y (2009) Advances in molecular genetics of cryptorchidism. Urology 74: 571–578.
43. Kojima Y, Kohri K, Hayashi Y (2010) Genetic pathway of external genitalia formation and molecular etiology of hypospadias. J Pediatr Urol 6: 346–354.
44. Rey RA, Codner E, Iniguez G, Bedecarras P, Trigo R, et al. (2005) Low risk of impaired testicular Sertoli and Leydig cell functions in boys with isolated hypospadias. J Clin Endocrinol Metab 90: 6035–6040.

Early Human Development 88 (2012) 517–523

Contents lists available at SciVerse ScienceDirect

Early Human Development

journal homepage: www.elsevier.com/locate/earlhumdev

Fetal myocardial tissue Doppler indices before birth physiologically change in proportion to body size adjusted for gestational age in low-risk term pregnancies

Katsuyuki Sekii [a,*], Takamichi Ishikawa [a], Tsutomu Ogata [a], Hiroaki Itoh [b], Satoru Iwashima [a]

[a] Department of Pediatrics, Hamamatsu University School of Medicine, Hamamatsu, Japan
[b] Department of Obstetrics and Gynecology, Hamamatsu University School of Medicine, Hamamatsu, Japan

ARTICLE INFO

Article history:
Received 3 November 2011
Accepted 17 December 2011

Keywords:
Cardiac function
Birth weight
z score
Pregnancy
Fetus
Placenta
Ultrasound

ABSTRACT

Background: Few studies have investigated the relationship between myocardial tissue Doppler parameters and fetal size adjusted for gestational age and its trend has been controversial.
Aims: To investigate fetal cardiac function before birth using tissue Doppler imaging (TDI: indicated by the prime symbol (′)) in low-risk term pregnancies by comparing the TDI parameters with gestational age-specific birth weight percentiles and z scores.
Study design and measurements
Interventricular septum, left and right ventricular myocardial peak early diastolic (E′), late diastolic (A′) and systolic (S′) velocities, E′/A′ ratios, myocardial performance index (MPI′) and umbilical artery pulsatility index were measured within three days before birth in 76 low-risk term pregnancies, including appropriate for gestational age (AGA, n = 50), small for gestational age (SGA, n = 10), and large for gestational age (LGA, n = 16) subjects.
Results: Myocardial peak velocities showed higher in the LGA and lower in the SGA compared with the AGA group, and All S′ positively correlated with birth weight (r = 0.51–0.57). All z scores of S′ demonstrated a positive correlation with birth weight z score (Spearman r = 0.45–0.53). MPI′ was significantly higher in the SGA and lower in the LGA compared with the AGA group. All MPI′ negatively correlated with birth weight (r = −0.55 to −0.65). All z scores of MPI′ showed a negative correlation with birth weight z score (Spearman r = −0.40 to −0.56).
Conclusions: Fetal myocardial peak velocities and MPI′ physiologically changed in proportion to body size adjusted for gestational age in low-risk term pregnancies.

1. Introduction

Tissue Doppler imaging (TDI: indicated by the prime symbol (′)) is an echocardiographic technique that uses Doppler principles to measure velocities and time intervals of myocardial motion in systole and diastole. TDI-derived myocardial peak velocities and myocardial performance index (MPI′) have been established as sensitive markers for early identification of heart failure observed in twin-to-twin transfusion syndrome, congenital heart defects or hydrops fetalis [1,2]. In addition, several studies have demonstrated the presence of echocardiographic and biochemical signs of subclinical cardiac dysfunction in some cases of fetal growth restriction [3–5]. Comas et al. have proposed that growth-restricted fetuses have significantly lower myocardial peak velocities and higher MPI′ values than normally grown fetuses, suggesting a higher sensitivity of TDI for detecting subclinical cardiac dysfunction in growth-restricted fetuses [6,7].

Association between fetal myocardial tissue Doppler parameters and gestational age has been investigated in the second and third trimesters of pregnancy [8]. Chan et al. proposed that fetal myocardial peak velocities increased with advancing gestational age and fetal cardiac function becomes increasingly mature in utero life during pregnancy [9]. Since fetal weight gradually increases with gestational age, these results indicate that the velocities increase in proportion to fetal weight as gestation proceeds. In normally grown fetuses, myocardial peak velocities positively correlate with estimated fetal weight independent of gestational age [10].

According to a recent opinion, Rasmussen has pointed out a possible clinical pitfall of using fetal weight-specific standards for myocardial tissue Doppler parameters in that it ignores information on gestational age [11]. If investigators assess the TDI parameters only based on fetal weight-specific reference charts without including gestational age, cardiac output in a growth-restricted fetus would simply mean a comparison with fetuses of the same size at earlier gestation. Similarly, cardiac output

* Corresponding author at: Department of Pediatrics, Hamamatsu University School of Medicine, 1-20-1 Handayama, Higashi-ku, Hamamatsu 431-3192, Japan. Tel.: +81 53 435 2312; fax: +81 53 435 2311.
E-mail address: sekii@hama-med.ac.jp (K. Sekii).

0378-3782/$ - see front matter © 2011 Elsevier Ireland Ltd. All rights reserved.
doi:10.1016/j.earlhumdev.2011.12.014

in an overgrown fetus would imply a comparison with fetuses at later gestation.

As far as we know, few studies have investigated the relationship between the TDI parameters and body size adjusted for gestational age, which is a percentile- and z score-based method of standardization for comparing body size measurements at each gestational age, although many fetal echocardiographic studies have only used the gestational age-specific percentile and z score to match or compare baseline measurements of body size between fetuses with normal and pathological conditions, such as maternal preeclampsia, fetal growth restriction and fetal heart failure [1,2,6,7,12]. In the present study, we measured fetal cardiac function using TDI within three days before birth in low-risk term pregnancies and compared the TDI parameters with gestational age, birth weight, gestational age-specific birth weight percentiles and z scores [13,14].

2. Methods

2.1. Study population

In this retrospective observational study, Japanese women with singleton pregnancies delivered at the Maternal–Fetal and Neonatal Care Center of Hamamatsu University School of Medicine between July 2010 and June 2011 were eligible. Gestational age was determined by ultrasound measurement of the fetal crown-rump length in the first-trimester. Normal fetal anatomy was confirmed by ultrasonography. Maternal and perinatal characteristics of the mother's age, parity, mode of delivery (vaginal or elective cesarean section), gestational age at birth, birth weight, neonatal sex, Apgar score and umbilical artery pH were recorded. Gestational age-specific birth weight z score (hereafter, 'birth weight z score') in SD units was calculated by the LMS method [13] in each case with Japanese gestational age-specific reference for birth weight [14]. The LMS method uses three parameters (L for the power in the Box–Cox transformation, M for the median, and S for the generalized coefficient of variation) to determine gestational age- and sex-specific z-scores for neonatal birth weight. After delivery, the placenta was weighed before trimming (the total placenta with the umbilical cord and membrane were weighed on digital scales).

Inclusion criteria for the study were live-birth singleton pregnancy between 37 and 41 weeks of gestation at birth without fetal malformations or hydrops fetalis. Ultrasound examination was carried out within three days before birth in all cases. Exclusion criteria included the following: women in active labor or rupture of membrane before fetal echocardiography, gestational or pre-gestational diabetes, preeclampsia [15], maternal disease (chronic hypertension, autoimmune disease), serological evidence of intrauterine infection, treatment with tocolytic drugs, uncertain gestational age, and cases in which not all echocardiographic parameters were recorded.

The study protocol was approved by the ethics committee of the Hamamatsu University School of Medicine. All participants gave written informed consent before voluntary enrolment.

2.2. Ultrasound examination

We used an HD11 XE ultrasound machine (Philips, Andover, MA, USA) equipped with a S8-3 Sector Array Transducer (3.0–8.0 MHz) for tissue Doppler echocardiography and a C5-2 Curved Array Transducer (2.0–5.0 MHz) to measure Doppler flow velocity of the umbilical artery. Image acquisition was performed by the same investigator (K. S.). Participants were examined in the supine or lateral decubitus positions, and the maximum duration for the ultrasonography was limited to 15 min in each case. All recordings were obtained in the absence of fetal movements and breathing movements, when the fetal heart rate was between 120 and 160 bpm. Fetal heart rate was calculated from the time interval between the onsets of the myocardial shortening velocity waveform during the ventricular systole in three consecutive cardiac cycles measured by TDI. The ultrasound beam was focused in the direction of the umbilical artery blood flow or the longitudinal myocardial wall motion as parallel as possible, and kept at an angle of less than 30°. No angle correction was used.

Doppler flow velocity waveforms of the umbilical artery were obtained from a free-floating loop of the umbilical cord. The monitor sweep speed was set at 35 mm/s and the filter was set at 100 Hz. The Doppler sample volume was set at 2.5 mm. Placental vascular impedance was assessed by calculating the umbilical artery pulsatility index (PI) values [3]. After obtaining a constant sequence of more than ten cycles, the average value of three consecutive cycles was used for further analysis.

The TDI program was set to pulsed-wave Doppler mode. Ventricular myocardial velocities were measured from the basal or apical four-chamber view. The monitor sweep speed was set at 100 mm/s and the wall filter was set at the lowest selection. A 2.9-mm Doppler sample volume was placed at the level of the interventricular septum, the lateral mitral annulus (left ventricular wall) and the lateral tricuspid annulus (right ventricular wall). The myocardial peak velocities during early diastole (E′), late diastole with atrial contraction (A′), and systole in the ejection phase (S′) were measured and the E′/A′ ratio was calculated. Time interval measurements were performed as follows: the time interval (a) was measured between the end of the A′ wave and the onset of the E′ wave. The time interval (b) was measured between the onset and the end of the S′ wave. The septum, left and right MPI′ values were calculated as: $(a-b)/b$. Each parameter was obtained from three consecutive cardiac cycles and the average value was used for further analysis [2].

2.3. Statistical analysis

The PASW statistics 18 (SPSS Inc., Chicago, IL, USA) were used for data analysis. All continuous variables were expressed as mean ± SD or median (min–max). Categorical data were given as counts (percentages). Pearson's correlation was used to assess the relationship between continuous variables. Spearman rank correlation was used to evaluate the relationship between z scores of myocardial tissue Doppler parameters and birth weight z score. Z scores (SD scores) of the TDI parameters were calculated using the following formula: $z=(V-M_V)/SD_V$, where V = measured TDI parameter, M_V = mean value for the TDI parameter and SD_V = SD for that TDI parameter. M_V and SD_V were calculated based on data from the study population.

To identify the relationship between echocardiographic parameters and gestational age-specific birth weight percentile groups, the study population was classified into three groups according to the Japanese gestational age-specific reference for birth weight based on the nationwide population [14] as follows: small for gestational age (SGA: birth weight is below the 10th percentile at gestational age), appropriate for gestational age (AGA: birth weight is between the 10th and 90th percentile at gestational age), or large for gestational age (LGA: birth weight is above the 90th percentile at gestational age). The statistical difference was determined by two-sided Student's *t* test. If the variables were not normally distributed, the Mann–Whitney's *U* test was chosen. The Chi-square test and Fisher's exact test were used for qualitative categorical analysis. $p<0.05$ was considered statistically significant.

3. Results

3.1. Characteristics of the study population

As a result of the exclusions, the present study included a total of 76 women with a singleton pregnancy. Seventy-six neonates were classified into three groups according to the Japanese gestational age-specific reference for birth weight [14] as follows: AGA group (n = 50), SGA group (n = 10) and LGA group (n = 16). Table 1

Table 1
Maternal, fetal, and perinatal characteristics of the study population classified into three groups according to Japanese gestational age-specific reference for birth weight [14].

	Total (n = 76)	AGA (n = 50)	SGA (n = 10)	LGA (n = 16)	P value[1]	P value[2]
Maternal age (years)	33.4 ± 4.8	33.6 ± 4.7	34.4 ± 4.7	32.0 ± 5.2	0.66	0.22
Primiparous woman (n (%))	22 (28.9)	17 (34.0)	1 (10.0)	4 (25.0)	0.13	0.50
Gestational age at ultrasound (weeks)	38.3 ± 1.1	38.4 ± 1.3	37.9 ± 0.6	38.0 ± 1.0	0.33	0.20
Gestational age at birth (weeks)	38.5 ± 1.1	38.6 ± 1.3	38.1 ± 0.6	38.2 ± 1.0	0.34	0.17
Interval between ultrasound and birth (days)	1 (0–3)	1 (0–3)	1.5 (1–3)	1 (1–2)	0.55	0.76
Cesarean delivery (n (%))	45 (59.2)	27 (54.0)	7 (70.0)	11 (68.8)	0.35	0.30
Male neonate (n (%))	38 (50.0)	27 (54.0)	4 (40.0)	7 (43.8)	0.42	0.48
Five-minute Apgar score	9 (8–10)	9 (8–10)	9 (9–10)	9 (9–10)	0.57	0.93
Umbilical artery pH	7.29 ± 0.06	7.30 ± 0.06	7.27 ± 0.07	7.29 ± 0.07	0.20	0.71
Birth weight (g)	2890 ± 406	2903 ± 233	2139 ± 186	3289 ± 271	**<0.001**	**<0.001**
Birth weight z score	0.21 ± 1.3	0.18 ± 0.70	−2.21 ± 0.64	1.74 ± 0.60	**<0.001**	**<0.001**
Placental weight (g)	542 ± 110	534 ± 75	385 ± 81	658 ± 81	**<0.001**	**<0.001**

Values are mean ± SD, n (%) or median (min–max). SGA: small-for-gestational age; AGA: appropriate-for-gestational age; LGA: large-for-gestational age; P value[1] = AGA versus SGA; P value[2] = AGA versus LGA. Significant p values (< 0.05) are given in bold type.

shows maternal, fetal and perinatal characteristics of each group. These were similar among the three groups with the exception of birth weight, birth weight z score and placental weight, which showed significant differences between groups ($p<0.001$, respectively).

3.2. Ultrasound examination

Fetal heart rate at ultrasound examination showed similar values in all three groups (137 ± 8 bpm in the AGA group, 136 ± 7 bpm in the SGA group and 138 ± 12 bpm in the LGA group).

Umbilical artery Doppler recordings showed no absent or reversed end-diastolic flow velocity waveforms in all three groups. Umbilical artery PI values were 0.87 ± 0.13 in the AGA group, 1.00 ± 0.22 in the SGA group and 0.83 ± 0.12 in the LGA group. The SGA group showed higher umbilical artery PI values than the AGA group ($p<0.01$). No differences were seen in umbilical artery PI values between the AGA and LGA groups. Umbilical artery PI demonstrated a negative correlation with birth weight and placental weight ($n=76$, $r=-0.34$ and $r=-0.30$, respectively; $p<0.01$).

Table 2 shows tissue Doppler parameters for all three ventricular walls in each group. Septum and left myocardial peak velocities except for left A′ values were significantly higher in the LGA group and lower in the SGA group as compared with the AGA group. Right E′, A′ and S′ values demonstrated lower in the SGA group than those in the AGA group. Right S′ values were significantly higher in the LGA group than those in the AGA group. Septum, left and right MPI′ values showed significantly higher in the SGA group than those in the AGA group ($p<0.001$, respectively). Septum and left MPI′ values were lower in the LGA group than those in the AGA group (septum; $p<0.001$ and left; $p<0.01$). In contrast, septum, left and right E′/A′ ratios showed similar values among the three groups.

We also examined the Pearson's correlation coefficients between tissue Doppler parameters and perinatal characteristics in the study population (Table 3). In all three ventricular walls, significant positive correlations were observed between E′ values and birth weight and placental weight. All A′ values positively correlated with birth weight. Septum and right A′ values showed a weak positive correlation with placental weight. All S′ values showed positive correlations with birth weight and placental weight ($r=0.51$–0.57 and $r=0.37$–0.53, respectively; $p<0.001$). Septum, left and right MPI′ values demonstrated a significant negative correlation with birth weight and placental weight ($r=-0.55$ to -0.65 and $r=-0.54$ to -0.76, respectively; $p<0.001$). There were no significant correlations between septum, left and right E′/A′ ratios and perinatal characteristics.

The relationship between z scores of the TDI parameters and birth weight z score was investigated in the study population with the Spearman rank correlation test. Figs. 1–3 show scatter plots of septum, left and right E′ (a), A′ (b), S′ (c) and MPI′ (d) z scores plotted against birth weight z score. In all three ventricular walls, z scores of myocardial peak velocities positively correlated with birth weight z score. Significant positive correlations were observed between all

Table 2
Tissue Doppler parameters in the study population classified into three groups according to Japanese gestational age-specific reference for birth weight [14].

	Total (n = 76)	AGA (n = 50)	SGA (n = 10)	LGA (n = 16)	P value[1]	P value[2]
Interventricular septum						
E′ (cm)	5.2 ± 1.2	5.2 ± 1.0	4.3 ± 1.2	5.8 ± 1.3	**<0.05**	**<0.05**
A′ (cm)	6.7 ± 1.7	6.6 ± 1.6	5.5 ± 1.0	7.4 ± 1.7	**<0.05**	**<0.05**
S′ (cm)	4.9 ± 0.7	4.9 ± 0.6	4.3 ± 0.5	5.4 ± 0.6	**<0.01**	**<0.05**
E′/A′	0.81 ± 0.22	0.81 ± 0.19	0.79 ± 0.23	0.82 ± 0.28	0.81	0.88
MPI′	0.50 ± 0.07	0.51 ± 0.05	0.61 ± 0.05	0.44 ± 0.06	**<0.001**	**<0.001**
Left ventricle						
E′ (cm)	7.0 ± 1.4	7.0 ± 1.0	5.9 ± 1.5	7.7 ± 2.0	**<0.01**	**<0.05**
A′ (cm)	8.0 ± 2.1	7.8 ± 2.0	7.0 ± 1.2	9.3 ± 2.0	0.23	**<0.05**
S′ (cm)	6.5 ± 0.9	6.6 ± 0.8	5.6 ± 0.5	7.0 ± 0.9	**<0.001**	**<0.05**
E′/A′	0.91 ± 0.22	0.93 ± 0.23	0.85 ± 0.20	0.85 ± 0.20	0.29	0.21
MPI′	0.51 ± 0.07	0.51 ± 0.06	0.60 ± 0.06	0.47 ± 0.06	**<0.001**	**<0.01**
Right ventricle						
E′ (cm)	8.3 ± 1.9	8.5 ± 1.9	6.7 ± 1.1	8.9 ± 1.8	**<0.01**	0.38
A′ (cm)	10.4 ± 2.3	10.4 ± 2.2	8.9 ± 1.5	11.2 ± 2.6	**<0.05**	0.22
S′ (cm)	6.9 ± 0.9	6.9 ± 0.9	6.0 ± 0.6	7.6 ± 0.7	**<0.01**	**<0.01**
E′/A′	0.82 ± 0.17	0.83 ± 0.17	0.76 ± 0.15	0.82 ± 0.18	0.23	0.75
MPI′	0.53 ± 0.07	0.52 ± 0.06	0.61 ± 0.06	0.49 ± 0.06	**<0.001**	0.09

Values are the mean ± SD. AGA: appropriate-for-gestational age; SGA: small-for-gestational age; LGA: large-for-gestational age; E′: myocardial peak velocity in early diastole; A′: myocardial peak velocity during atrial contraction; S′: myocardial peak velocity in systole; MPI′: myocardial performance index measured by tissue Doppler imaging; P value[2] = AGA versus SGA; P value[2] = AGA versus LGA. Significant p values (< 0.05) are given in bold type.

Table 3
Pearson's correlation coefficient between tissue Doppler parameters and perinatal characteristics in the study population (n = 76).

	Interventricular septum			Left ventricle			Right ventricle		
	GA at ultrasound	Birth weight	Placental weight	GA at ultrasound	Birth weight	Placental weight	GA at ultrasound	Birth weight	Placental weight
E′	0.10	0.41‡	0.31†	−0.01	0.28†	0.24*	0.07	0.34†	0.25*
A′	0.15	0.35†	0.33†	0.09	0.25*	0.15	0.04	0.35†	0.24*
S′	0.19	0.57‡	0.53‡	0.20	0.51‡	0.37‡	0.18	0.51‡	0.40‡
E′/A′	−0.11	0.04	−0.03	−0.10	0.03	0.08	0.04	0.04	0.06
MPI′	−0.20	−0.65‡	−0.76‡	−0.10	−0.59‡	−0.70‡	−0.18	−0.55‡	−0.54‡

GA: gestational age; E′: myocardial peak velocity in early diastole; A′: myocardial peak velocity during atrial contraction; S′: myocardial peak velocity in systole; MPI′: myocardial performance index measured by tissue Doppler imaging. *$p<0.05$; †$p<0.01$; ‡$p<0.001$.

S′ z scores and birth weight z score (Spearman rho = 0.45–0.53, $p<0.001$). Septum, left and right MPI′ z scores showed a significant negative correlation with birth weight z score (Spearman rho = −0.40 to −0.56, $p<0.001$). In contrast, there were no correlations between birth weight z score and septum (Spearman rho = 0.03, $p=0.83$), left (Spearman rho = 0.04, $p=0.73$), or right (Spearman rho = −0.08, $p=0.48$) E′/A′ ratio z scores.

4. Discussion

In the present study, we compared fetal myocardial tissue Doppler parameters within three days before birth with both gestational age-specific birth weight percentile groups and birth weight z scores, according to the recent opinion of Rasmussen [11]. As far as we know, the present study is the first to assess the relationships between the TDI parameters and birth weight adjusted for gestational age in low-risk term pregnancies. The results suggest significant differences between the percentile groups in myocardial peak velocities and MPI′. Z scores of the TDI parameters show a significant correlation with birth weight z score. These findings indicate that myocardial peak velocities and MPI′ vary according to body size adjusted for gestational age in term fetuses.

Myocardial peak velocities showed higher in the LGA group and lower in the SGA group as compared with the AGA group, and the velocities positively correlated with birth weight (Tables 2, 3). Similar tendencies were seen in the relationship between z scores of the velocities and birth weight z score (Figs. 1–3). The findings support the proposal that fetal myocardial peak velocities positively correlate with fetal body size [10] and SGA fetuses have lower myocardial peak velocities than normally grown fetuses [7]. In addition, several studies of adult hearts may give clues to the mechanistic background of the findings. Myocardial peak velocities have a tendency to increase in healthy adults with large left ventricular mass and/or cavity size [16–18]. Anatomical assessment indicated that the reference values for fetal cardiac weight linearly increased in proportion to actual body weight throughout the second and third trimesters [19–21].

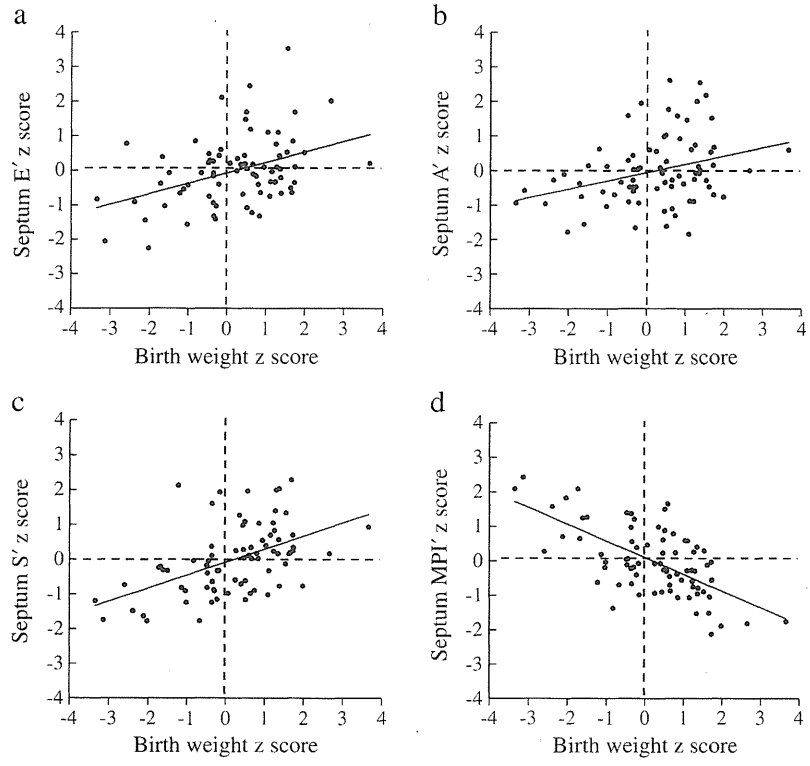

Fig. 1. Relationship between z scores of interventricular septum myocardial tissue Doppler parameters and birth weight z score in the study population (n = 76). There were positive correlations between (a) septum E′ z score (Spearman rho = 0.34, $p<0.01$), (b) septum A′ z score (Spearman rho = 0.32, $p<0.01$) and (c) septum S′ z score (Spearman rho = 0.53, $p<0.001$) and birth weight z score. There were negative correlations between (d) septum MPI′ z score and birth weight z score (Spearman rho = −0.56, $p<0.001$). E′: myocardial peak velocity in early diastole; A′: myocardial peak velocity during atrial contraction; S′: myocardial peak velocity in systole; MPI′: myocardial performance index measured by tissue Doppler imaging.

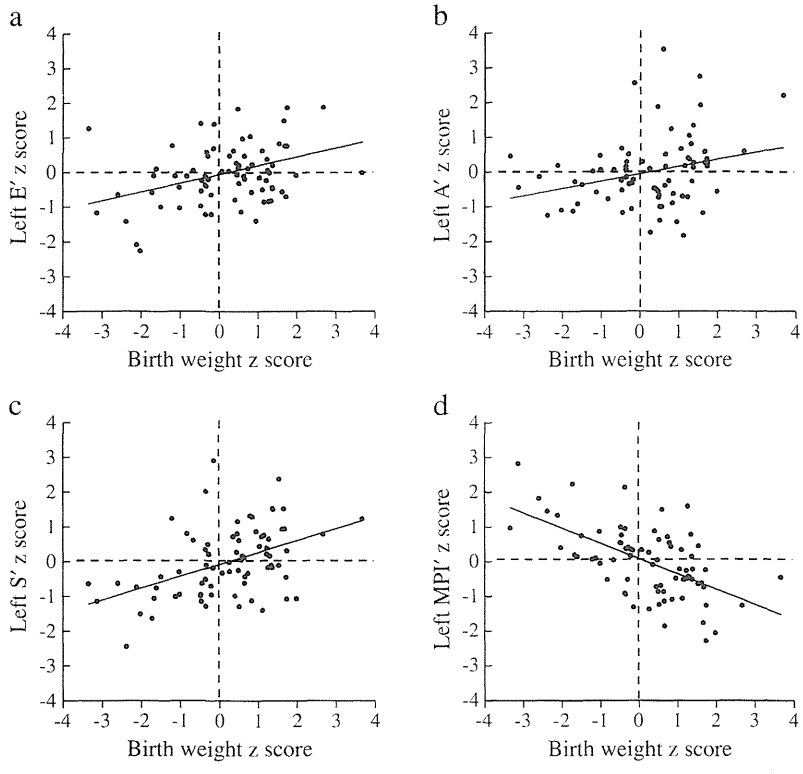

Fig. 2. Relationship between z scores of left ventricular myocardial tissue Doppler parameters and birth weight z score in the study population (n = 76). There were positive correlations between (a) left E′ z score (Spearman rho = 0.31, p<0.01), (b) left A′ z score (Spearman rho = 0.29, p<0.05) and (c) left S′ z score (Spearman rho = 0.45, p<0.001) and birth weight z score. There were negative correlations between (d) left MPI′ z score and birth weight z score (Spearman rho = −0.53, p<0.001). E′: myocardial peak velocity in early diastole; A′: myocardial peak velocity during atrial contraction; S′: myocardial peak velocity in systole; MPI′: myocardial performance index measured by tissue Doppler imaging.

Miyague and Ghidini showed that AGA, as well as SGA, fetuses have a positive correlation between estimated fetal weight and ultrasound measurement of heart circumference and area [22]. It is plausible that the variations in myocardial peak velocities represent the physiological difference in fetal cardiac size or fetal body size based on gestational age.

The MPI′ showed significantly higher in the SGA group and lower in the LGA group as compared with the AGA group and negatively correlated with birth weight (Tables 2, 3). Moreover, a strong negative correlation was observed between MPI′ z score and birth weight z score (Figs. 1–3). These results indicate that MPI′ decrease in proportion to body size adjusted for gestational age. The findings support the view that SGA fetuses have higher MPI′ than normally grown fetuses at term gestation, although Comas et al. have proposed that the differences in MPI′ between normal and SGA fetuses are due to the presence of subclinical cardiac dysfunction in SGA fetuses [7]. Interestingly, it was reported that MPI′ values were independent of body size in healthy infants, children and adolescents [23,24]. At present, we have no clear explanation regarding the discrepancy.

Several investigators have proposed that the undesirable changes in the TDI parameters observed in growth-restricted fetuses indicate the presence of subclinical cardiac dysfunction [6–8]. However, our findings support the hypothesis that the relatively low myocardial peak velocities with high MPI′ in SGA fetuses may lead to overestimation in the presence of subclinical cardiac dysfunction. On the contrary, the relatively high myocardial peak velocities with low MPI′ in LGA fetuses may lead to underestimation. Indeed, at 0–24 and 96–120 h after birth, septum, and left and right MPI′ values were in the normal range of cardiac function in the three groups, and there were no significant differences in the MPI′ between the groups (unpublished observations). Since few studies have explored the relationship between myocardial tissue Doppler parameters and fetal size adjusted for gestational age, it would be useful to establish cut-off values for the TDI parameters based on fetal size in each gestational age.

In the present study, the umbilical artery PI showed a weak negative correlation with birth weight and placental weight (r = −0.34 and r = −0.34, respectively). In contrast, the MPI′ had a strong negative correlation with birth weight as well as placental weight (r = −0.55 to −0.65 and r = −0.54 to −0.76, respectively). The placenta is one of the largest fetal organs [21]. Approximately one third of fetal cardiac output flows reach the placental vascular bed in preterm and term pregnant sheep [25,26], suggesting a considerable contribution of the feto-placental unit to fetal cardiac function. In an experimental model of pathophysiological status of placenta, Acharya et al. demonstrated that embolization of ovine placenta did not affect fetal cardiac output and umbilical artery PI [27]. However, the present study suggests that the entire size of placental vascular bed could affect fetal cardiac function at least in physiological status. Therefore, further studies are in progress concerning a possible association between physiological changes in the placental vascular bed and fetal cardiac function.

Our data suggest that myocardial tissue Doppler parameters have no significant correlations with gestational age in low-risk term pregnancies. The findings, especially E′, A′ and S′ values, are inconsistent with the proposal that myocardial peak velocities positively correlated with gestational age between mid-gestation and term [9,10]. The discrepancy may be explained by the fact that the present study was composed of only term fetuses. Exclusion of preterm fetuses from the study population may diminish the correlation between the TDI parameters and gestational age at ultrasound.

There are some limitations to the present study. First, we did not estimate the fetal weight at the ultrasound examination, and could

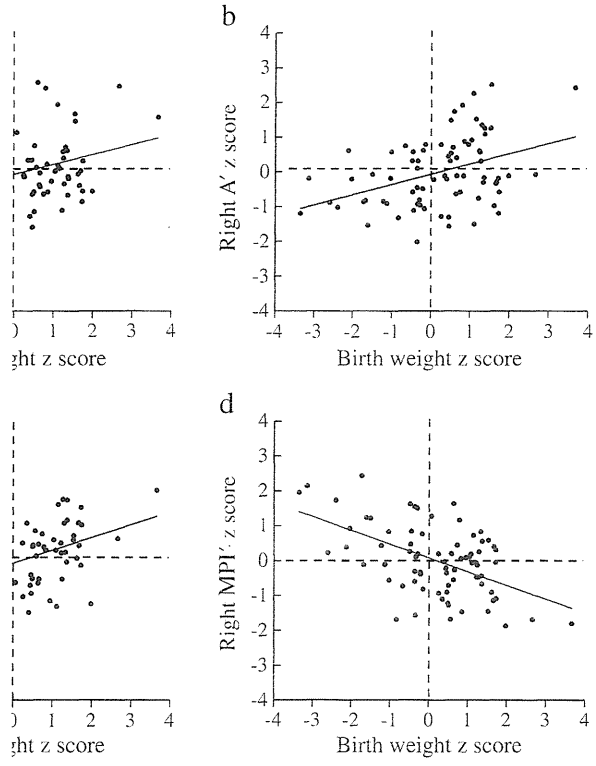

dial tissue Doppler parameters and birth weight z score in the study population (n = 76). There were positive cor-
0.01), (b) right A' z score (Spearman rho = 0.35, p<0.01) and (c) right S' z score (Spearman rho = 0.46, p<0.001)
en (d) right MPI' z score and birth weight z score (Spearman rho = −0.40, p<0.001). E': myocardial peak velocity
raction; S': myocardial peak velocity in systole; MPI': myocardial performance index measured by tissue Doppler

eight. Second, ap-
ere through elec-
tions. Since most
) weeks' gestation
r rates of cesarean
an gestational age
Third, the results
of SGA or LGA fe-
with pathological
rowth restriction
going concerning
ises with normal

ncreased and the
v-risk term preg-
between z scores
se results suggest
ppler parameters
cardiac function

tential conflict of
ork.

Sources of funding

There were no external funding sources for this study.

References

[1] Watanabe S, Hashimoto I, Saito K, Watanabe K, Hirono K, Uese K, et al. Characterization of ventricular myocardial performance in the fetus by tissue Doppler imaging. Circ J 2009;73:943–7.
[2] Acharya G, Pavlovic M, Ewing L, Nollmann D, Leshko J, Huhta JC. Comparison between pulsed-wave Doppler- and tissue Doppler-derived Tei indices in fetuses with and without congenital heart disease. Ultrasound Obstet Gynecol 2008;31:406–11.
[3] Mäkikallio K, Vuolteenaho O, Jouppila P, Räsänen J. Ultrasonographic and biochemical markers of human fetal cardiac dysfunction in placental insufficiency. Circulation 2002;105:2058–63.
[4] Girsen A, Ala-Kopsala M, Makikallio K, Vuolteenaho O, Rasanen J. Cardiovascular hemodynamics and umbilical artery N-terminal peptide of proB-type natriuretic peptide in human fetuses with growth restriction. Ultrasound Obstet Gynecol 2007;29:296–303.
[5] Crispi F, Hernandez-Andrade E, Pelsers MM, Plasencia W, Benavides-Serralde JA, Eixarch E, et al. Cardiac dysfunction and cell damage across clinical stages of severity in growth-restricted fetuses. Am J Obstet Gynecol 2008;199:254.e1–8.
[6] Comas M, Crispi F, Cruz-Martinez R, Martinez JM, Figueras F, Gratacós E. Usefulness of myocardial tissue Doppler vs conventional echocardiography in the evaluation of cardiac dysfunction in early-onset intrauterine growth restriction. Am J Obstet Gynecol 2010;203:45.e1–7.
[7] Comas M, Crispi F, Cruz-Martinez R, Figueras F, Gratacós E. Tissue Doppler echocardiographic markers of cardiac dysfunction in small-for-gestational age fetuses. Am J Obstet Gynecol 2011;205:57.e1–6.
[8] Larsen LU, Petersen OB, Sloth E, Uldbjerg N. Color Doppler myocardial imaging demonstrates reduced diastolic tissue velocity in growth retarded fetuses with flow redistribution. Eur J Obstet Gynecol Reprod Biol 2011;155:140–5.
[9] Chan LY, Fok WY, Wong JT, Yu CM, Leung TN, Lau TK. Reference charts of gestation-specific tissue Doppler imaging indices of systolic and diastolic functions in the normal fetal heart. Am Heart J 2005;150:750–5.

[10] Comas M, Crispi F, Gómez O, Puerto B, Figueras F, Gratacós E. Gestational age- and estimated fetal weight-adjusted reference ranges for myocardial tissue Doppler indices at 24–41 weeks' gestation. Ultrasound Obstet Gynecol 2011;37:57–64.
[11] Rasmussen S. Charts to assess fetal wellbeing. Ultrasound Obstet Gynecol 2011;37:2–5.
[12] Naujorks AA, Zielinsky P, Beltrame PA, Castagna RC, Petracco R, Busato A, et al. Myocardial tissue Doppler assessment of diastolic function in the growth-restricted fetus. Ultrasound Obstet Gynecol 2009;34:68–73.
[13] Cole TJ, The LMS. Method for constructing normalized growth standards. Eur J Clin Nutr 1990;44:45–60.
[14] Itabashi K, Fujimura M, Kusuda S, Tamura M, Hayashi T, Takahashi T, et al. Introduction of new gestational age-specific standards for birth size. J Jpn Pediatr Soc 2010;114:1271–93.
[15] Minakami H, Hiramatsu Y, Koresawa M, Fujii T, Hamada H, Iitsuka Y, et al. Guidelines for obstetrical practice in Japan: Japan Society of Obstetrics and Gynecology (JSOG) and Japan Association of Obstetricians and Gynecologists (JAOG) 2011 edition. J Obstet Gynaecol Res 2011;37:1174–97.
[16] Tümüklü MM, Ildizli M, Ceyhan K, Cinar CS. Alterations in left ventricular structure and diastolic function in professional football players: assessment by tissue Doppler imaging and left ventricular flow propagation velocity. Echocardiography 2007;24:140–8.
[17] Pelà G, Bruschi G, Montagna L, Manara M, Manca C. Left and right ventricular adaptation assessed by Doppler tissue echocardiography in athletes. J Am Soc Echocardiogr 2004;17:205–11.
[18] Zoncu S, Pelliccia A, Mercuro G. Assessment of regional systolic and diastolic wall motion velocities in highly trained athletes by pulsed wave Doppler tissue imaging. J Am Soc Echocardiogr 2002;15:900–5.
[19] Oyer CE, Sung CJ, Friedman R, Hansen K, Paepe MD, Pinar H, et al. Reference values for valve circumferences and ventricular wall thicknesses of fetal and neonatal hearts. Pediatr Dev Pathol 2004;7:499–505.
[20] Velozo LF, Segovia LA, Zapata LA, Peralta S, Rodriguez NA. Measurements of valve circumferences and ventricular wall of fetal hearts in Chile. Pediatr Dev Pathol 2010;13:95–100.
[21] Nakayama M, Arai H, Takeuchi M, Nakamura Y, Takeshima S, Kimoto A. Organ weights, cardiac size in infancy along with placental size and weight. J Osaka Med Cent Res Inst Matern Child Health 1997;13:103–15.
[22] Miyague NI, Ghidini A. Effect of fetal growth restriction on ultrasonographically measured cardiac size. Early Hum Dev 1997;48:93–8.
[23] Cui W, Roberson DA, Chen Z, Madronero LF, Cuneo BF. Systolic and diastolic time intervals measured from Doppler tissue imaging: normal values and Z-score tables, and effects of age, heart rate, and body surface area. J Am Soc Echocardiogr 2008;21:361–70.
[24] Eidem BW, McMahon CJ, Cohen RR, Wu J, Finkelshteyn I, Kovalchin JP, et al. Impact of cardiac growth on Doppler tissue imaging velocities: a study in healthy children. J Am Soc Echocardiogr 2004;17:212–21.
[25] Baschat AA, Gembruch U. Development of fetal cardiac and extracardiac Doppler flows in early gestation. In: Yagel S, Silverman NH, Gembruch U, editors. Fetal Cardiology. Second ed. New York: Informa Healthcare; 2008. p. 153–71.
[26] Rudolph AM. Distribution and regulation of blood flow in the fetal and neonatal lamb. Circ Res 1985;57:811–21.
[27] Acharya G, Erkinaro T, Mäkikallio K, Lappalainen T, Räsänen J. Relationships among Doppler-derived umbilical artery absolute velocities, cardiac function, and placental volume blood flow and resistance in fetal sheep. Am J Physiol Heart Circ Physiol 2004;286:H1266–72.

Journal of Human Genetics (2012) 57, 449–452

www.nature.com/jhg

ORIGINAL ARTICLE

Haplotype analysis of *ESR2* in Japanese patients with spermatogenic failure

Tsutomu Ogata[1,2], Maki Fukami[2], Rie Yoshida[2], Eiko Nagata[1], Yasuko Fujisawa[1], Atsumi Yoshida[3] and Yasunori Yoshimura[4]

The prevalence of spermatogenic failure (SF) has gradually increased during the past few decades at least in several countries. Although multiple factors would be involved in this phenomenon, one important factor would be excessive estrogen effects via estrogen receptors (ERs). Thus, we performed haplotype analysis of *ESR2* encoding ERβ in 125 Japanese SF patients and 119 age-matched control males, using single nucleotide polymorphisms (SNPs) 1–9 that are widely distributed on the ~120-kb genomic sequence of *ESR2*. Consequently, a linkage disequilibrium (LD) block was detected in an ~60-kb region encompassing SNPs 2–7 in both groups, and four major estimated haplotypes were identified within the LD block. Furthermore, the most prevalent 'TGTAGA' haplotype was found to be significantly associated with SF, with the *P*-value obtained by the Cochran–Armitage trend test (0.0029) being lower than that obtained by a 100 000-times permutation test (0.0038) to cope with the problem of multiple comparisons. The results, in conjunction with our previous data indicating lack of a susceptibility factor on *ESR1* encoding ERα, imply that the specific 'TGTAGA' haplotype of *ESR2* raises the susceptibility to the development of SF.
Journal of Human Genetics (2012) **57**, 449–452; doi:10.1038/jhg.2012.53; published online 24 May 2012

Keywords: environmental endocrine disruptors; *ESR2*; estrogenic effects; haplotype analysis; spermatogenic failure; susceptibility

INTRODUCTION

Recent studies have indicated a gradual increase in the prevalence of male genial and reproductive abnormalities during the past few decades at least in several countries.[1] Skakkebaek *et al.*[2] have coined a term 'testicular dysgenesis syndrome' for this phenomenon. As such deterioration of male genital and reproductive health is also observed in many wildlife species,[1,3] it is likely that such adverse changes in males are inter-related events shared in common by the human and the wildlife species.[1,3] In this regard, environmental endocrine disruptors (EEDs) appear to constitute the major factor for this phenomenon, because EEDs are widely spread in the world.[1,3] In particular, exposure to estrogenic EEDs are known to affect male genital and reproductive health.[1,3–5]

The effects of EEDs would primarily be determined by the genetic susceptibility, together with the dosage of exposed EEDs, character of exposed EEDs (for example, estrogenic, anti-androgenic and so on), and the developmental stage of the individuals at the time of EED exposure.[1,3] In this regard, it is known that estrogenic EEDs can bind to both estrogen receptor (ER)α encoded by *ESR1* and ERβ encoded by *ESR2* with low but variable degrees of affinities.[3] Thus, it is likely that genetic susceptibility to estrogenic EEDs is primarily constituted by genetic variations in *ESR1* and *ESR2*.[1,3]

To examine this possibility, we have previously performed haplotype analysis of *ESR1* in Japanese male patients with genial and reproductive abnormalities as well as in control males, using 15 single nucleotide polymorphisms (SNPs 1–15) that are widely distributed throughout the >300-kb genomic sequence of *ESR1*.[6,7] Consequently, we identified an ~50-kb linkage disequilibrium (LD) block spanning SNPs 10–14 in the 3′ region of *ESR1*, and found that homozygosity of a specific 'AGATA' haplotype within the LD block was strongly associated with cryptorchidism ($P = 0.0040$; odds ratio (OR) = 7.55) and hypospadias ($P = 0.000057$; OR = 13.75)[6,7] (and our unpublished updated observation). This finding provides strong evidence that homozygosity of the specific *ESR1* haplotype raises the susceptibility to the development of male genital abnormalities. In this context, we speculate that this effect via the specific *ESR1* haplotype is mediated by EEDs, although there is no direct evidence yet. Indeed, as *ESR1* is expressed in Leydig cells producing testosterone and insulin-like 3,[5,8] it is likely that the specific *ESR1* haplotype primarily enhances estrogenic effects in Leydig cells, compromising their hormonal production capacity.

However, no significant association was found between the specific 'AGATA' haplotype of *ESR1* and spermatogenic failure (SF).[7] In this context, as *ESR2* is clearly expressed in various developmental stages of male germ cells,[5] it may be possible that the deleterious effects of estrogenic EEDs on spermatogenesis may primarily be mediated by ERβ. Thus, we carried out haplotype analysis of *ESR2* in Japanese patients with SF.

[1]Department of Pediatrics, Hamamatsu University School of Medicine, Hamamatsu, Japan; [2]Department of Molecular Endocrinology, National Research Institute for Child Health and Development, Tokyo, Japan; [3]Kiba Park Clinic, Tokyo, Japan and [4]Department of Obstetrics and Gynecology, Keio University School of Medicine, Tokyo, Japan
Correspondence: Professor T Ogata, Department of Pediatrics, Hamamatsu University School of Medicine, 1-20-1, Handayama, Higashi-ku, Hamamatsu, Shizuoka 431-3192, Japan.
E-mail: tomogata@hama-med.ac.jp
Received 28 November 2011; revised 25 April 2012; accepted 28 April 2012; published online 24 May 2012

MATERIALS AND METHODS

Subjects

We studied 125 SF patients aged 32–52 years (median 41.0 years), including 80 SF patients utilized in the previous *ESR1* haplotype analysis.[7] The selection criteria included: (1) azoospermia or severe oligozoospermia (<5 million sperms per ml) demonstrated by two consecutive analyses of semen obtained after 4–7 days of abstinence; (2) lack of extragenital anomalies such as cryptorchidism and hypospadias; (3) hypergonadotropic hypogonadism indicative of primary testicular dysfunction; (4) no seminal tract obstruction, varicocele, or retrograde ejaculation; (5) a 46,XY karyotype with no demonstrable structural or numerical abnormality after examining ⩾30 lymphocytes; (6) absence of a Y chromosomal microdeletion after examining 36 loci from *SRY* to *DYZ1*, including multiple Yq loci in the azoospermia factor regions (AZFa, b, c) such as *RBMY* and *DAZ*;[9] (7) no significant expansion of CAG repeat length at exon 1 of *AR* that is known to raise the susceptibility to male reproductive abnormalities;[10] and (8) lack of a disease episode that could affect fertility such as mumps orchiditis. For controls, 119 control adult males with proven fertility aged 24–50 years (median 35.5 year) were similarly analyzed with permission. The ages were similar between the SF patients and control males (Mann–Whitney's *U*-test). All the SF patients and control males were Japanese living in the Tokyo urban area; they were free from particular residential environments such as the vicinity of chemical factories or farms, from specific dietary habits deviated to vegetables or animal/fish proteins, and from intake of drugs with hormonal effects.

SNP analysis

This study was approved by the Institutional Review Board Committees of the authors, and informed consent was obtained from each subject. We examined nine SNPs (SNPs 1–9) that were associated with high minor allele frequencies in the Japanese population (20.3–39.5%) (the NCBI Short Genetic Variations Database (dbSNP); http://www.ncbi.nlm.nih.gov/snp/) and were widely distributed on the ~120-kb *ESR2* genomic DNA sequence including an apparent LD block encompassing exons 1–6 identified in various populations (the International HapMap Project Database; http://hapmap.ncbi.nlm.nih.gov/) (Figure 1a). Genotyping was performed by the 5′ nuclease assay on an ABI PRISM 7000 Sequence Detection System (Life Technologies, Carlsbad, CA, USA),[11] using leukocyte genomic DNA of each subject.

Pearson's χ^2-test with one degree of freedom was applied to test whether the genotyping data are in the Hardy–Weinberg equilibrium. Statistical significance of the differences in allele and genotype frequencies was analyzed by Pearson's χ^2-test, using R environment for statistical computing (http://www.r-project.org/).

Haplotype analysis

Although haplotypes are usually not observed, the haplotypes present in a subject and the frequencies of the haplotypes in a population can be inferred using genotype data at separate loci.[12] In this regard, the degree of LD can be expressed as the pairwise $|D'|$ value (the absolute value for the disequilibrium parameter) that ranges from 0 (complete absence of LD) to 1.0 (complete presence of LD),[13] and a chromosomal region associated with high $|D'|$ values between different loci is defined as a haplotype or an LD block.[14] In this study, haplotype inference was performed by the maximum-likelihood method using expectation maximization algorithm implemented in the software LDSUPPORT.[15,16] The pairwise $|D'|$ values were estimated by the method of Terwilliger and Ott, [12] and a haplotype block was determined by the method of Zhu *et al.*[17] using the software developed by Kamatani *et al.*[18]

The difference in the frequencies of haplotypes between the SF patients and the control males was examined using the estimated population haplotype frequencies by Pearson's χ^2-test, and the OR and the 95% confidence interval (CI) were calculated using the R environment. The association between SF phenotype and estimated haplotypes was tested using PENHAPLO software in a dominant mode (comparison of the frequencies of subjects with one risk haplotype between cases and controls) and in a recessive mode (comparison of the frequencies of subjects with two risk haplotypes between cases and controls).[19] Furthermore, the association between SF phenotype and estimated haplotypes was also examined in a dosage-dependent mode (comparison of the frequencies of subjects with zero, one, and two risk haplotypes between cases and controls) by the Cochran–Armitage trend test,[20,21] using the R environment. To cope with the problem of multiple comparisons, the significant level was determined by a 100 000-times permutation test.[22]

RESULTS

SNP analysis

The results of SNP analysis are summarized in Table 1. Minor allele frequencies of the 9 SNPs were 20.4–46.8% in the SF patients and 27.7–37.3% in control males. The genotype frequencies of SNPs 1–9 were in accord with the Hardy–Weinberg equilibrium. Low *P*-values (<0.05) were identified for the differences in the allele and genotype frequencies of SNPs 1, 4, and 5, with stronger association being identified for the

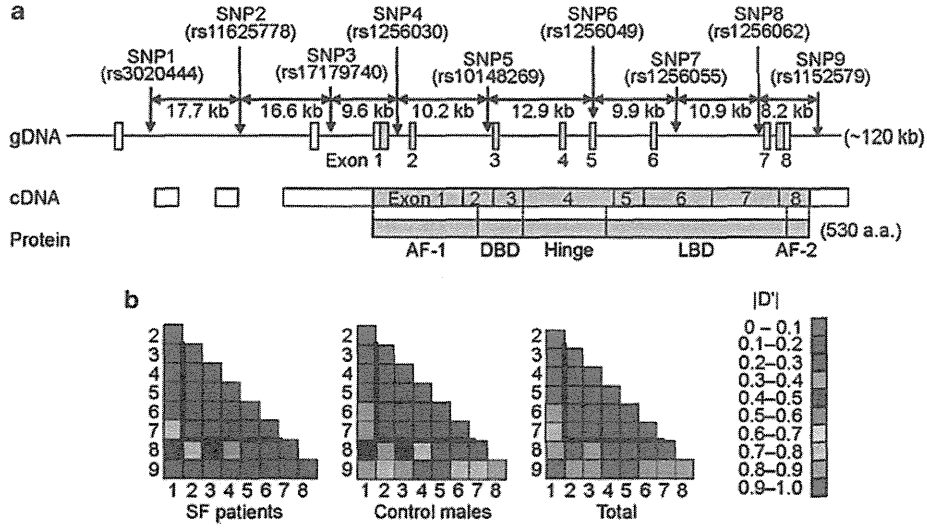

Figure 1 Schematic representation of *ESR2* and its LD maps. **(a)** Physical positions of *ESR2* SNPs 1–9 examined in the present study. The gray and the white boxes represent coding and untranslated regions, respectively. AF-1, activation function 1 (ligand independent); AF-2: activation function 2 (ligand dependent); DBD, DNA-binding domain; LBD, ligand-binding domain. **(b)** Pairwise LD maps. $|D'|$: an absolute value for the disequilibrium parameter.

Table 1 Summary of SNP analysis

Genotyping data				*Statistical data*			
	Genotype	*SF*	*CM*		*P-value*	*OR*	*95% CI*
SNP1	TT	78	58	T vs C	0.028	1.59	1.05–2.42
rs3020444	TC	43	53	TT vs TC + CC	0.032	0.57	0.34–0.95
	CC	4	8	TT + TC vs CC	0.20	2.18	0.64–7.44
SNP2	TT	68	63	T vs C	0.74	1.07	0.72–1.56
rs11625778	TC	48	46	TT vs TC + CC	0.82	0.94	0.57–1.56
	CC	9	10	TT + TC vs CC	0.73	1.18	0.46–3.02
SNP3	GG	77	59	G vs A	0.059	1.49	0.98–2.25
rs17179740	AG	43	52	GG vs AG + AA	0.059	0.61	0.37–1.02
	AA	5	8	GG + AG vs AA	0.34	1.73	0.55–5.45
SNP4	CC	36	55	C vs T	0.0022	1.77	1.23–2.56
rs1256030	CT	61	49	CC vs CT + TT	0.0049	2.13	1.25–3.61
	TT	28	15	CC + CT vs TT	0.045	0.500	0.25–0.99
SNP5	GG	36	55	G vs A	0.0022	1.77	1.23–2.56
rs10148269	AG	61	49	GG vs AG + AA	0.0049	2.13	1.25–3.61
	AA	28	15	GG + AG vs AA	0.045	0.500	0.25–0.99
SNP6	GG	68	64	G vs A	0.74	1.07	0.72–1.60
rs1256049	GA	49	45	GG vs GA + AA	0.92	0.98	0.59–1.61
	AA	8	10	GG + GA vs AA	0.55	1.34	0.51–3.52
SNP7	AA	68	64	A vs G	0.74	1.07	0.72–1.60
rs1256055	AG	49	45	AA vs AG + GG	0.92	0.98	0.59–1.61
	GG	8	10	AA + AG vs GG	0.55	1.34	0.51–3.52
SNP8	AA	59	47	A vs G	0.21	1.27	0.87–1.85
rs1256062	AG	54	57	AA vs AG + GG	0.22	0.73	0.44–1.21
	GG	12	15	AA + AG vs GG	0.45	1.36	0.61–3.04
SNP9	GG	40	45	G vs A	0.12	1.34	0.93–1.92
rs1152579	GA	59	59	GG vs GA + AA	0.34	1.29	0.76–2.19
	AA	26	15	GG + GA vs AA	0.087	0.55	0.28–1.10

Abbreviations: CI, confidence interval; OR, odds ratio; SNP, single nucleotide polymorphism. NCBI rs no. is given for each SNP. SF, 125 patients with spermatogenic failure; CM, 119 control males.

allele rather than the genotype frequencies. In particular, the *P*-values for allele frequencies of SNPs 4 and 5 were markedly low.

Haplotype analysis

The LD map is shown in Figure 1b, and the results of haplotype analysis are summarized in Table 2. An ~60-kb LD block spanning SNPs 2–7 was identified in both the SF patients and control males, with the $|D'|$ value being >0.9 for all the pairs of SNPs 2–7. Within the LD block, four major estimated haplotypes were identified, together with three additional minor haplotypes ('CGTAGA' haplotype in a single control male, and 'TATAGA' and 'CGCGGA' haplotypes in single SF patients). Notably, the frequency of the most prevalent 'TGTAGA' haplotype was significantly higher in the SF patients than in the control males. Furthermore, the 'TGTAGA' haplotype was significantly associated with SF phenotype, with the *P*-value obtained by the Cochran–Armitage trend test (0.0029) being lower than the permutation *P*-value (0.0038). In addition, of the four major haplotypes, the 'TGTAGA' haplotype alone contained the 'T' allele in SNP 4 and the 'A' allele in SNP 5, whereas these two alleles were also identified in two of the three minor haplotypes.

DISCUSSION

The present study revealed the presence of an ~60-kb LD block encompassing SNPs 2–7 of *ESR2* in both the SF patients and control males. In this regard, the allele frequencies obtained in the control males are comparable to those registered in the JSNP Database, and the LD block identified in this study is similar to that reported in the International HapMap Project. These findings argue for the accuracy of our data.

Table 2 Summary of haplotype analysis (SNPs 2–7)

Estimated haplotype	*TGTAGA*	*TACGGA*	*CGCGAG*	*TGCGGA*
SF ($n=125$)	46.4%	21.2%	26.0%	6.0%
CM ($n=119$)	32.7%	28.1%	27.3%	11.0%
Comparison of estimated haplotype frequency				
P-value	0.0028	0.096	0.82	0.070
OR	1.77	0.69	0.94	0.52
95% CI	1.21–2.61	0.44–1.06	0.61–1.43	0.25–1.05
Association of estimated haplotype with phenotype				
Dominant mode				
P-value	0.0063	0.078	0.92	0.031
OR	2.08	0.63	0.98	0.46
95% CI	1.23–3.54	0.38–1.05	0.59–1.62	0.22–0.93
Recessive mode				
P-value	0.026	0.34	0.55	0.97
OR	2.16	0.58	0.75	0.95
95% CI	1.09–4.46	0.17–1.79	0.28–1.96	0.037–24.2
Cochran–Armitage's trend test				
P-value	0.0029	0.071	0.75	0.056
For one haplotype				
OR	1.75	0.67	0.94	0.52
95% CI	1.21–2.52	0.44–1.03	0.63–1.39	0.27–1.02
For two haplotypes				
OR	3.06	0.45	0.88	0.27
95% CI	1.46–6.35	0.19–1.06	0.39–1.93	0.07–1.04

Abbreviations: CI, confidence interval; OR, odds ratio; SNP, single nucleotide polymorphism. SF, 125 patients with spermatogenic failure; CM, 119 control males.

Of the four major estimated haplotypes within the LD block, the 'TGTAGA' haplotype was significantly associated with SF. Indeed, the *P*-value obtained by the Cochran–Armitage trend test was below the permutation *P*-value. Furthermore, comparison of the *P*-values obtained from the three types of analyses for the association between SF phenotype and estimated haplotypes implies that the specific 'TGTAGA' haplotype compromises spermatogenesis in a dosage-dependent manner rather than in a simple dominant or recessive manner. In this regard, as the 'T' allele of SNP 4 and the 'A' allele of SNP 5 are almost exclusively present in the 'TGTAGA' haplotype, genotyping of SNPs 4 and 5 can be utilized for the screening of the 'TGTAGA' haplotype.

For *ESR2*, previous studies have suggested an association between SF and an *Rsa*I SNP on exon 5 that does not result in amino acid change (SNP 6 in this study) in Scandinavian and Iranian populations (*P*-value: 0.01 and 0.012, respectively).[23,24] In such studies, as the frequency of AG genotype relative to GG genotype was higher in SF patients than in control males (AA genotype was extremely rare), this would imply that the 'A' allele of SNP 6 is regarded as a marker for a hidden true susceptibility factor(s) that is probably in an LD status with the 'A' allele of SNP 6. By contrast, the present study showed no association of SF with SNP 6 and rather suggests a dosage effect of the specific haplotype harboring the 'G' allele of SNP 6. Thus, the present data are apparently inconsistent with the previous studies. It might be possible, however, that the true susceptibility factor(s) is linked with the specific 'TGTAGA' haplotype in the Japanese population and resides on a different pattern of haplotype carrying the 'A' allele of SNP 6 in Scandinavian and Iranian populations, because of a recombination between the true susceptibility factor(s) and SNP 6 in either of the ethnic groups. In addition, there might be population-

specific susceptibility factors, and false positive results might be obtained in association studies with multiple comparisons. This matter awaits further studies.

One may argue that although the present study indicates an association of the specific *ESR2* haplotype with SF, there is no direct evidence for estrogenic EEDs being involved in the development of SF. Indeed, it may be possible that an interaction between the specific *ESR2* haplotype and endogenous estrogens rather than estrogenic EEDs actually underlie the development of SF. However, estrogenic effects of EEDs are known to be primarily mediated by ER.[1,3] In addition, as all the SF patients and the control males examined in this study were apparently free from high exposure to EEDs, the amount of exposed EEDs would be similar between the two groups of subjects. Thus, although further studies such as the investigation of subjects with a high risk of EEDs exposure (for example, workers at chemical factories) are necessary, our results would suggest that the specific *ESR2* haplotype constitutes a susceptibility factor for the development of SF in response to estrogenic EEDs in males who live in an ordinary condition with no high risk of EEDs exposure.

Several points should be made with respect to the present study. First, the number of subjects analyzed remains rather small. Second, the true susceptibility factor(s) on the specific haplotype remains to be identified, although the specific 'TGTAGA' haplotype would facilitate the development of SF by enhancing the ERβ signaling. Third, it remains possible that another susceptibility factor(s) is present on *ESR2*. In particular, as only a few of SNPs were examined in non-LD block regions, a different susceptibility factor(s) may be present on the non-LD block regions of *ESR2*. Fourth, several patients may have some unidentified pathologic cause(s) for SF such as single gene disorders. Fifth, there may be some unknown minor genetic and environmental differences between the patients and the control males. In this context, as SF becomes discernible in adulthood, such minor differences, if they exist, may exert unfavorable influences on spermatogenic function for a long time, leading to SF. This may explain why the OR obtained in this study remained low, in contrast to the high ORs identified in cryptorchidism (7.55) and hypospadias (13.75)[6,7] (and our unpublished updated observation) which develop during the fetal life. Sixth, although it is known that EEDs also exert anti-androgenic effects and influence aromatization,[25,26] these have not been examined in this study. Lastly, it remains to be determined whether similar results can be reproduced in other case–control studies.

Despite the above caveats, this study provides a useful clue to clarify the genetic susceptibility to estrogenic EEDs. In summary, we propose that the specific *ESR2* haplotype raises the susceptibility to the development of SF in response to estrogenic EEDs. Further studies including similar haplotype analyses in different ethnic groups from both developed and developing countries will serve to clarify the relative importance of the dosage of exposed EEDs and the genetic heterogeneity obtained in the process of natural human selection, in the presumably EEDs-related phenomenon such as SF.

CONFLICT OF INTEREST

The authors declare no conflict of interest.

ACKNOWLEDGEMENTS

We would like to thank Dr Kamitsuji at StaGen Co., Ltd. for his critical advice in the genetic statistical analyses. This study was supported in part by the Environment Research and Technology Development Fund (C-0905) of the Ministry of Environment, by the Grants for Research on Intractable Diseases (H22-098), Health Research on Children, Youth and Families (H21–005), and Research on Risk of Chemical Materials (H20-004) from the Ministry of Health, Labor and Welfare, by the Grants-in-Aid for Scientific Research (S) (22227002) from the Japan Society for the Promotion of Science (JSPS), and Grant-in-Aid for Scientific Research on Innovative Areas (22132004) from the Ministry of Education, Culture, Sports, Science and Technology (MEXT), and by the Grant from National Center for Child Health and Development (20C-2).

1 Toppari, J., Larsen, J. C., Christiansen, P., Giwercman, A., Grandjean, P., Guillette, Jr. L. J. *et al.* Male reproductive health and environmental xenoestrogens. *Environ. Health Perspect.* **104,** (Suppl 4) 741–803 (1996).
2 Skakkebaek, N. E., Rajpert-De Meyts, E. & Main, K. M. Testicular dysgenesis syndrome: an increasingly common developmental disorder with environmental aspects. *Hum. Reprod.* **16,** 972–978 (2001).
3 McLachlan, J. A. Environmental signaling: what embryos and evolution teach us about endocrine disrupting chemicals. *Endocr. Rev.* **22,** 319–341 (2001).
4 Stillman, R. J. *In utero* exposure to diethylstilbestrol: adverse effects on the reproductive tract and reproductive performance and male and female offspring. *Am. J. Obstet. Gynecol.* **142,** 905–921 (1982).
5 O'Donnell, L., Robertson, K. M., Jones, M. E. & Simpson, E. R. Estrogen and spermatogenesis. *Endocr. Rev.* **22,** 289–318 (2001).
6 Yoshida, R., Fukami, M., Sasagawa, I., Hasegawa, T., Kamatani, N. & Ogata, T. Association of cryptorchidism with a specific haplotype of the estrogen receptor alpha gene: implication for the susceptibility to estrogenic environmental endocrine disruptors. *J. Clin. Endocrinol. Metab.* **90,** 4716–4721 (2005).
7 Watanabe, M., Yoshida, R., Ueoka, K., Aoki, K., Sasagawa, I., Hasegawa, T. *et al.* Haplotype analysis of the estrogen receptor 1 gene in male genital and reproductive abnormalities. *Hum. Reprod.* **22,** 1279–1284 (2007).
8 Foresta, C., Zuccarello, D., Garolla, A. & Ferlin, A. Role of hormones, genes, and environment in human cryptorchidism. *Endocr. Rev.* **29,** 560–580 (2008).
9 Vogt, P. H. AZF deletions and Y chromosomal haplogroups: history and update based on sequence. *Hum. Reprod. Update* **11,** 319–336 (2005).
10 Dowsing, A. T., Yong, E. L., Clark, M., McLachlan, R. I., de Kretser, D. M. & Trouson, A. O. Linkage between male infertility and trinucleotide repeat expansion in the androgen-receptor gene. *Lancet* **354,** 640–643 (1999).
11 De La Vega, F. M., Dailey, D., Ziegle, J., Williams, J., Madden, D. & Gilbert, D. A. New generation pharmacogenomic tools: a SNP linkage disequilibrium map, validated SNP assay resource, and high-throughput instrumentation system for large-scale genetic studies. *Biotechniques* **32,** S48–S54 (2002).
12 Terwilliger, J. D. & Ott, J. *Handbook of Human Genetic Linkage* (Johns Hopkins University Press, Baltimore, 1994).
13 Lewontin, R. C. The interaction of selection and linkage. I. General considerations: heterotic models. *Genetics* **49,** 49–67 (1964).
14 Kruglyak, L. Prospects for whole-genome linkage disequilibrium mapping of common disease genes. *Nat. Genet.* **22,** 139–144 (1999).
15 Excoffier, L. & Slatkin, M. Maximum-likelihood estimation of molecular haplotype frequencies in a diploid population. *Mol. Biol. Evol.* **12,** 921–927 (1995).
16 Kitamura, Y., Moriguchi, M., Kaneko, H., Morisaki, H., Morisaki, T., Toyama, K. *et al.* Determination of probability distribution of diplotype configuration (diplotype distribution) for each subject from genotypic data using the EM algorithm. *Ann. Hum. Genet.* **66,** 183–193 (2002).
17 Zhu, X., Yan, D., Cooper, R. S., Luke, A., Ikeda, M. A., Chang, Y. P. *et al.* Linkage disequilibrium and haplotype diversity in the genes of the renin-angiotensin system: findings from the family blood pressure program. *Genome Res.* **13,** 173–181 (2003).
18 Kamatani, N., Sekine, A., Kitamoto, T., Iida, A., Saito, S., Kogame, A. *et al.* Large scale single-nucleotide polymorphism (SNP) and haplotype analyses, using dense SNP maps, of 199 drug-related genes in 752 subjects: the analysis of the association between uncommon SNPs within haplotype blocks and the haplotypes constructed with haplotype-tagging SNPs. *Am. J. Hum. Genet* **75,** 190–203 (2004).
19 Ito, T., Inoue, E. & Kamatani, N. Association test algorithm between a qualitative phenotype and a haplotype or haplotype set using simultaneous estimation of haplotype frequencies, diplotype configurations, and diplotype-based penetrances. *Genetics* **168,** 2339–2348 (2004).
20 Cochran, W. G. Some methods for strengthening the common chi-square tests. *Biometrics* **10,** 417–451 (1954).
21 Armitage, P. Tests for Linear Trends in Proportions and Frequencies. *Biometrics* **11,** 375–386 (1955).
22 Becker, T. & Knapp, M. A powerful strategy to account for multiple testing in the context of haplotype analysis. *Am. J. Hum. Genet* **75,** 561–570 (2004).
23 Aschim, E. L., Giwercman, A., Ståhl, O., Eberhard, J., Cwikiel, M., Nordenskjöld, A. *et al.* The *Rsa*I polymorphism in the estrogen receptor-beta gene is associated with male infertility. *J. Clin. Endocrinol. Metab.* **90,** 5343–5348 (2005).
24 Safarinejad, M. R., Shafiei, N. & Safarinejad, S. Association of polymorphisms in the estrogen receptors alpha, and beta (ESR1, ESR2) with the occurrence of male infertility and semen parameters. *J. Steroid Biochem. Mol. Biol* **122,** 193–203 (2010).
25 Svechnikov, K., Izzo, G., Landreh, L., Weisser, J. & Soder, O. Endocrine disruptors and Leydig cell function. *J. Biomed. Biotechnol* **2010,** 684504 (2010).
26 Whitehead, S. A. & Rice, S. Endocrine-disrupting chemicals as modulators of sex steroid synthesis. *Best Pract. Res. Clin. Endocrinol. Metab* **20,** 45–61 (2006).

PRKAR1A Mutation Affecting cAMP-Mediated G Protein-Coupled Receptor Signaling in a Patient with Acrodysostosis and Hormone Resistance

Keisuke Nagasaki, Tomoko Iida, Hidetoshi Sato, Yohei Ogawa, Toru Kikuchi, Akihiko Saitoh, Tsutomu Ogata, and Maki Fukami

Department of Molecular Endocrinology (K.N., T.O., M.F.), National Research Institute for Child Health and Development, Tokyo 157-8535, Japan; Division of Pediatrics (K.N., H.S., Y.O., T.K., A.S.), Department of Homeostatic Regulation and Development, Niigata University Graduate School of Medical and Dental Sciences, Niigata, 951-8510, Japan; Department of Pediatrics (T.I.), Niigata National Hospital, Niigata, 945-8585, Japan; and Department of Pediatrics (T.O.), Hamamatsu University School of Medicine, Hamamatsu 431-3192, Japan

Context: Acrodysostosis is a rare autosomal dominant disorder characterized by short stature, peculiar facial appearance with nasal hypoplasia, and short metacarpotarsals and phalanges with cone-shaped epiphyses. Recently, mutations of *PRKAR1A* and *PDE4D* downstream of *GNAS* on the cAMP-mediated G protein-coupled receptor (GPCR) signaling cascade have been identified in acrodysostosis with and without hormone resistance, although functional studies have been performed only for p.R368X of *PRKAR1A*.

Objective: Our objective was to report a novel *PRKAR1A* mutation and its functional consequence in a Japanese female patient with acrodysostosis and hormone resistance.

Patient: This patient had acrodysostosis-compatible clinical features such as short stature and brachydactyly and mildly elevated serum PTH and TSH values.

Results: Although no abnormality was detected in *GNAS* and *PDE4D*, a novel *de novo* heterozygous missense mutation (p.T239A) was identified at the cAMP-binding domain A of *PRKAR1A*. Western blot analysis using primary antibodies for the phosphorylated cAMP-responsive element (CRE)-binding protein showed markedly reduced CRE-binding protein phosphorylation in the forskolin-stimulated lymphoblastoid cell lines of this patient. CRE-luciferase reporter assays indicated significantly impaired response of protein kinase A to cAMP in the HEK293 cells expressing the mutant p.T239A protein.

Conclusions: The results indicate that acrodysostosis with hormone resistance is caused by a heterozygous mutation at the cAMP-binding domain A of *PRKAR1A* because of impaired cAMP-mediated GPCR signaling. Because *GNAS*, *PRKAR1A*, and *PDE4D* are involved in the GPCR signal transduction cascade and have some different characters, this would explain the phenotypic similarity and difference in patients with *GNAS*, *PRKAR1A*, and *PDE4D* mutations. **(*J Clin Endocrinol Metab* 97: E1808–E1813, 2012)**

Acrodysostosis is a rare autosomal dominant disorder characterized by short stature, peculiar facial appearance with nasal hypoplasia, short metacarpotarsals and phalanges with cone-shaped epiphyses, and variable degrees of mental retardation (1, 2). Recent studies have shown that acrodysostosis is caused by mutations of *PRKAR1A* (protein

ISSN Print 0021-972X ISSN Online 1945-7197
Printed in U.S.A.

doi: 10.1210/jc.2012-1369 Received February 9, 2012. Accepted May 25, 2012.
First Published Online June 20, 2012

Abbreviations: AHO, Albright's hereditary osteodystrophy; CRE, cAMP-responsive element; CREB, CRE-binding; DMR, differentially methylated regions; GNAS, stimulatory G protein α-subunit; GPCR, G protein-coupled receptor; PDE4D, phosphodiesterase 4D, cAMP-specific; PHP-Ia, pseudohypoparathyroidism type Ia; PKA, protein kinase A; PRKAR1A, protein kinase, cAMP-dependent, regulatory type 1,α; RIα, type 1α regulatory subunit.